arXiv:1412.4092v1 [hep-ex] 12 Dec 2014

Centrality and rapidity dependence of inclusive jet production in $\sqrt{s_{\mathrm{NN}}} = 5.02\,\mathrm{TeV}$ proton–lead collisions with the ATLAS detector

The ATLAS Collaboration

Abstract

Measurements of the centrality and rapidity dependence of inclusive jet production in $\sqrt{s_{\mathrm{NN}}} = 5.02\,\mathrm{TeV}$ proton–lead (p+Pb) collisions and the jet cross-section in $\sqrt{s} = 2.76\,\mathrm{TeV}$ proton–proton collisions are presented. These quantities are measured in datasets corresponding to an integrated luminosity of $27.8\,\mathrm{nb}^{-1}$ and $4.0\,\mathrm{pb}^{-1}$, respectively, recorded with the ATLAS detector at the Large Hadron Collider in 2013. The p+Pb collision centrality was characterised using the total transverse energy measured in the pseudorapidity interval $-4.9 < \eta < -3.2$ in the direction of the lead beam. Results are presented for the double-differential per-collision yields as a function of jet rapidity and transverse momentum (p_{T}) for minimum-bias and centrality-selected p+Pb collisions, and are compared to the jet rate from the geometric expectation. The total jet yield in minimum-bias events is slightly enhanced above the expectation in a p_{T}-dependent manner but is consistent with the expectation within uncertainties. The ratios of jet spectra from different centrality selections show a strong modification of jet production at all p_{T} at forward rapidities and for large p_{T} at mid-rapidity, which manifests as a suppression of the jet yield in central events and an enhancement in peripheral events. These effects imply that the factorisation between hard and soft processes is violated at an unexpected level in proton–nucleus collisions. Furthermore, the modifications at forward rapidities are found to be a function of the total jet energy only, implying that the violations may have a simple dependence on the hard parton–parton kinematics.

Centrality and rapidity dependence of inclusive jet production in $\sqrt{s_{\mathrm{NN}}} = 5.02$ TeV proton–lead collisions with the ATLAS detector

ATLAS Collaboration

Abstract

Measurements of the centrality and rapidity dependence of inclusive jet production in $\sqrt{s_{\mathrm{NN}}} = 5.02$ TeV proton–lead (p+Pb) collisions and the jet cross-section in $\sqrt{s} = 2.76$ TeV proton–proton collisions are presented. These quantities are measured in datasets corresponding to an integrated luminosity of 27.8 nb^{-1} and 4.0 pb^{-1}, respectively, recorded with the ATLAS detector at the Large Hadron Collider in 2013. The p+Pb collision centrality was characterised using the total transverse energy measured in the pseudorapidity interval $-4.9 < \eta < -3.2$ in the direction of the lead beam. Results are presented for the double-differential per-collision yields as a function of jet rapidity and transverse momentum (p_{T}) for minimum-bias and centrality-selected p+Pb collisions, and are compared to the jet rate from the geometric expectation. The total jet yield in minimum-bias events is slightly enhanced above the expectation in a p_{T}-dependent manner but is consistent with the expectation within uncertainties. The ratios of jet spectra from different centrality selections show a strong modification of jet production at all p_{T} at forward rapidities and for large p_{T} at mid-rapidity, which manifests as a suppression of the jet yield in central events and an enhancement in peripheral events. These effects imply that the factorisation between hard and soft processes is violated at an unexpected level in proton–nucleus collisions. Furthermore, the modifications at forward rapidities are found to be a function of the total jet energy only, implying that the violations may have a simple dependence on the hard parton–parton kinematics.

1. Introduction

Proton–lead (p+Pb) collisions at the Large Hadron Collider (LHC) provide an excellent opportunity to study hard scattering processes involving a nuclear target [1]. Measurements of jet production in p+Pb collisions provide a valuable benchmark for studies of jet quenching in lead–lead collisions by, for example, constraining the impact of nuclear parton distributions on inclusive jet yields. However, p+Pb collisions also allow the study of possible violations of the factorisation between hard and soft processes in collisions involving nuclei.

Previous studies in deuteron–gold (d+Au) collisions at the Relativistic Heavy Ion Collider (RHIC) observed such violations, manifested in the suppressed production of very forward hadrons with transverse momenta up to 4 GeV [2–4]. Studies of forward dihadron angular correlations at RHIC also showed a much weaker dijet signal in d+Au collisions than in pp collisions [4,5]. These effects have been attributed to the saturation of the parton

distributions in the gold nucleus [6–8], to the modification of the nuclear parton distribution function [9], to the higher-twist contributions to the cross-section enhanced by the forward kinematics of the measurement [10], or to the presence of a large nucleus [11]. The extended kinematic reach of p+Pb measurements at the LHC allows the study of hard scattering processes that produce forward hadrons or jets over a much wider rapidity and transverse momentum range. Such measurements can determine whether the factorisation violations observed at RHIC persist at higher energy and, if so, how the resulting modifications vary as a function of particle or jet momentum and rapidity. The results of such measurements could test the competing descriptions of the RHIC results and, more generally, provide new insight into the physics of hard scattering processes involving a nuclear target.

This paper reports the centrality dependence of inclusive jet production in p+Pb collisions at a nucleon–nucleon centre-of-mass energy $\sqrt{s_{\mathrm{NN}}} = 5.02$ TeV. The measurement was performed using a

dataset corresponding to an integrated luminosity of 27.8 nb^{-1} recorded in 2013. The p+Pb jet yields were compared to a nucleon–nucleon reference constructed from a measurement of jet production in pp collisions at a centre-of-mass energy $\sqrt{s} = 2.76$ TeV using a dataset corresponding to an integrated luminosity of 4.0 pb^{-1} also recorded in 2013. Jets were reconstructed from energy deposits measured in the calorimeter using the anti-k_t algorithm with radius parameter $R = 0.4$ [12].

The centrality of p+Pb collisions was characterised using the total transverse energy measured in the pseudorapidity[1] interval $-4.9 < \eta < -3.2$ in the direction of the lead beam. Whereas in nucleus–nucleus collisions centrality reflects the degree of nuclear overlap between the colliding nuclei, centrality in p+Pb collisions is sensitive to the multiple interactions between the proton and nucleons in the lead nucleus. Centrality has been successfully used at lower energies in d+Au collisions at RHIC as an experimental handle on the collision geometry [13,14].

A Glauber model [15] was used to determine the average number of nucleon–nucleon collisions, $\langle N_{\text{coll}} \rangle$, and the mean value of the overlap function, $T_{pA}(b) = \int_{-\infty}^{+\infty} \rho(b, z) \mathrm{d}z$, where $\rho(b, z)$ is the nucleon density at impact parameter b and longitudinal position z, in each centrality interval. Per-event jet yields, $(1/N_{\text{evt}})(\mathrm{d}^2 N_{\text{jet}}/\mathrm{d}p_{\text{T}}\mathrm{d}y^*)$, were measured as a function of jet centre-of-mass rapidity,[2] y^*, and transverse momentum, p_{T}, where N_{jet} is the number of jets measured in N_{evt} p+Pb events analysed. The centrality dependence of the per-event jet yields was evaluated using the nuclear modification factor,

$$R_{p\text{Pb}} \equiv \frac{1}{T_{pA}} \frac{(1/N_{\text{evt}})\ \mathrm{d}^2 N_{\text{jet}}/\mathrm{d}p_{\text{T}}\mathrm{d}y^*\big|_{\text{cent}}}{\mathrm{d}^2 \sigma_{\text{jet}}^{pp}/\mathrm{d}p_{\text{T}}\mathrm{d}y^*}, \quad (1)$$

for a given centrality selection "cent", where $\mathrm{d}^2\sigma_{\text{jet}}^{pp}/\mathrm{d}p_{\text{T}}\mathrm{d}y^*$ is determined using the jet cross-section measured in pp collisions at $\sqrt{s} = 2.76$ TeV. The factor $R_{p\text{Pb}}$ quantifies the absolute modification of the jet rate relative to the geometric expectation. In each centrality interval, the geometric expectation is the jet rate that would be produced by an incoherent superposition of the number of nucleon–nucleon collisions corresponding to the mean nuclear thickness in the given class of p+Pb collisions.

Results are also presented for the central-to-peripheral ratio,

$$R_{\text{CP}} \equiv \frac{1}{R_{\text{coll}}} \frac{(1/N_{\text{evt}})\ \mathrm{d}^2 N_{\text{jet}}/\mathrm{d}p_{\text{T}}\mathrm{d}y^*\big|_{\text{cent}}}{(1/N_{\text{evt}})\ \mathrm{d}^2 N_{\text{jet}}/\mathrm{d}p_{\text{T}}\mathrm{d}y^*\big|_{\text{peri}}}, \quad (2)$$

where R_{coll} represents the ratio of $\langle N_{\text{coll}} \rangle$ in a given centrality interval to that in the most peripheral interval, $R_{\text{coll}} \equiv \langle N_{\text{coll}}^{\text{cent}} \rangle / \langle N_{\text{coll}}^{\text{peri}} \rangle$. The R_{CP} ratio is sensitive to relative deviations in the jet rate from the geometric expectation between the p+Pb event centralities. The $R_{p\text{Pb}}$ and R_{CP} measurements are presented as a function of inclusive jet y^* and p_{T}.

For the 2013 p+Pb run, the LHC was configured with a 4 TeV proton beam and a 1.57 TeV per-nucleon Pb beam that together produced collisions with $\sqrt{s_{\text{NN}}} = 5.02$ TeV and a rapidity shift of the centre-of-mass frame of 0.465 units relative to the ATLAS rest frame. The run was split into two periods, with the directions of the proton and lead beams being reversed at the end of the first period. The first period provided approximately 55% of the integrated luminosity with the Pb beam travelling to positive rapidity and the proton beam to negative rapidity, and the second period provided the remainder with the beams reversed. The analysis in this paper uses the events from both periods of data-taking and y^* is defined so that $y^* > 0$ always refers to the downstream proton direction.

2. Experimental setup

The measurements presented in this paper were performed using the ATLAS inner detector (ID), calorimeters, minimum-bias trigger scintillator (MBTS), and trigger and data acquisition

---

[1]ATLAS uses a right-handed coordinate system with its origin at the nominal interaction point (IP) in the centre of the detector and the z-axis along the beam pipe. The x-axis points from the IP to the centre of the LHC ring, and the y-axis points upward. Cylindrical coordinates (r, ϕ) are used in the transverse plane, ϕ being the azimuthal angle around the beam pipe. The pseudorapidity is defined in laboratory coordinates in terms of the polar angle θ as $\eta = -\ln\tan(\theta/2)$. During 2013 p+Pb data taking, the beam directions were reversed approximately half-way through the running period, but in presenting results the direction of the proton beam is always chosen to point to positive η.

[2]The jet rapidity y^* is defined as $y^* = 0.5 \ln \frac{E+p_z}{E-p_z}$ where E and p_z are the energy and the component of the momentum along the proton beam direction in the nucleon–nucleon centre-of-mass frame.

systems [16]. The ID measures charged particles within $|\eta| < 2.5$ using a combination of silicon pixel detectors, silicon microstrip detectors, and a straw-tube transition radiation tracker, all immersed in a 2 T axial magnetic field [17]. The calorimeter system consists of a liquid argon (LAr) electromagnetic (EM) calorimeter covering $|\eta| < 3.2$, a steel/scintillator sampling hadronic calorimeter covering $|\eta| < 1.7$, a LAr hadronic calorimeter covering $1.5 < |\eta| < 3.2$, and two LAr electromagnetic and hadronic forward calorimeters (FCal) covering $3.2 < |\eta| < 4.9$. The EM calorimeters use lead plates as the absorbers and are segmented longitudinally in shower depth into three compartments with an additional presampler layer in front for $|\eta| < 1.8$. The granularity of the EM calorimeter varies with layer and pseudorapidity. The middle sampling layer, which typically has the largest energy deposit in EM showers, has a $\Delta\eta \times \Delta\phi$ granularity of 0.025×0.025 within $|\eta| < 2.5$. The hadronic calorimeter uses steel as the absorber and has three segments longitudinal in shower depth with cell sizes $\Delta\eta \times \Delta\phi = 0.1 \times 0.1$ for $|\eta| < 2.5$[3] and 0.2×0.2 for $2.5 < |\eta| < 4.9$. The two FCal modules are composed of tungsten and copper absorbers with LAr as the active medium, which together provide ten interaction lengths of material. The MBTS detects charged particles over $2.1 < |\eta| < 3.9$ using two hodoscopes of 16 counters each, positioned at $z = \pm 3.6\,\mathrm{m}$.

The p+Pb and pp events used in this analysis were recorded using a combination of minimum-bias (MB) and jet triggers [18]. In p+Pb data-taking, the MB trigger required hits in at least one counter in each side of the MBTS detector. In pp collisions the MB condition was the presence of hits in the pixel and microstrip detectors reconstructed as a track by the high level trigger system. Jets were selected using high-level jet triggers implemented with a reconstruction algorithm similar to that applied in the offline analysis. The high-level jet triggers were seeded from a combination of low-level MB and jet hardware-based triggers. Multiple jet triggers with transverse energy thresholds ranging from 20 GeV to 75 GeV were used with prescales that varied with time to accommodate the evolution of the luminosity within an LHC fill.

---

[3]An exception is the third (outermost) sampling layer, which has a segmentation of 0.2×0.1 up to $|\eta| = 1.7$.

3. Data selection

In the offline analysis, charged-particle tracks were reconstructed in the ID using an algorithm optimised for pp minimum-bias measurements [19]. The p+Pb events used for this analysis were required to have a reconstructed vertex containing at least two associated tracks with $p_\mathrm{T} > 0.1$ GeV, at least one hit in each of the two MBTS hodoscopes, and a difference between times measured on the two MBTS sides of less than 10 ns. Events containing multiple p+Pb collisions (pileup) were suppressed by rejecting events having two or more reconstructed vertices, each associated with reconstructed tracks with a total transverse momentum scalar sum of at least 5 GeV. The fraction of events with one p+Pb interaction rejected by this requirement was less than 0.1%. Events with a pseudorapidity gap (defined by the absence of clusters in the calorimeter with more than 0.2 GeV of transverse energy) of greater than two units on the Pb-going side of the detector were also removed from the analysis. Such events arise primarily from electromagnetic or diffractive excitation of the proton. After accounting for event selection, the number of p+Pb events sampled by the highest-luminosity jet trigger (which was unprescaled) was 53 billion. The event selection criteria described here were designed to select a sample of p+Pb events to which a centrality analysis can be applied and for which meaningful geometric parameters can be determined.

The pp events used in this analysis were required to have a reconstructed vertex, with the same definition as the vertices in p+Pb events above. No other requirements were applied.

4. Centrality determination

The centrality of the p+Pb events selected for analysis was characterised by the total transverse energy $\Sigma E_\mathrm{T}^\mathrm{Pb}$ in the FCal module on the Pb-going side. The $\Sigma E_\mathrm{T}^\mathrm{Pb}$ distribution for minimum-bias p+Pb collisions passing the event selection described in Section 3 is presented in Fig. 1. Following standard techniques [20], centrality intervals were defined in terms of percentiles of the $\Sigma E_\mathrm{T}^\mathrm{Pb}$ distribution after accounting for an estimated inefficiency of $(2 \pm 2)\,\%$ for inelastic p+Pb collisions to pass the applied event selection. The following centrality intervals were used in this analysis, in order from the most central to the most peripheral: 0–10%, 10–20%, 20–30%, 30–40%, 40–60%, and 60–90%, with
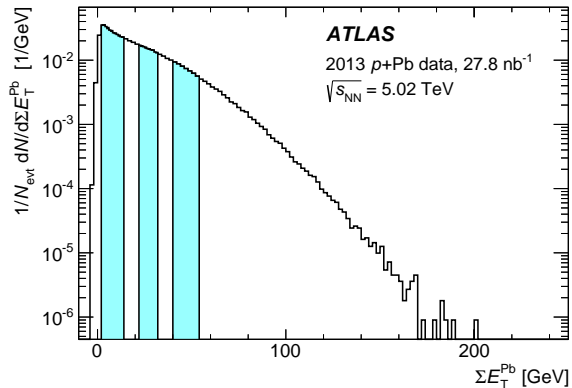
Fig. 1: Distribution of $\Sigma E_{\mathrm{T}}^{\mathrm{Pb}}$ for minimum-bias p+Pb collisions recorded during the 2013 run, measured in the FCal at $-4.9 < \eta < -3.2$ in the Pb-going direction. The vertical divisions correspond to the six centrality intervals used in this analysis. From right to left, the regions correspond to centrality intervals of 0–10%, 10–20%, 20–30%, 30–40%, 40–60% and 60–90%.

the 60–90% interval serving as the reference in the R_{CP} ratio.

A Glauber Monte Carlo (MC) [15] analysis was used to calculate R_{coll} and $T_{p\mathrm{A}}$ for each centrality interval. First, a Glauber MC program [21] was used to simulate the geometry of inelastic p+Pb collisions and calculate the probability distribution of the number of nucleon participants N_{part}, $P(N_{\mathrm{part}})$. The simulations used a Woods–Saxon nuclear density distribution and an inelastic nucleon–nucleon cross-section, σ_{NN}, of 70 ± 5 mb. Separately, PYTHIA [22,23] simulations of 4 TeV on 1.57 TeV pp collisions (using version 8.150, with generator parameters chosen to reproduce observables according to the so-called 4C tune [24], and incorporating the MSTW2008LO set of parton distribution functions [25]) provided a detector-level $\Sigma E_{\mathrm{T}}^{\mathrm{Pb}}$ distribution for nucleon–nucleon collisions, to be used as input to the Glauber model. This distribution was fit to a gamma distribution.

Then, an extension of the wounded-nucleon (WN) [26] model that included a non-linear dependence of $\Sigma E_{\mathrm{T}}^{\mathrm{Pb}}$ on N_{part} was used to define N_{part}-dependent gamma distributions for $\Sigma E_{\mathrm{T}}^{\mathrm{Pb}}$, with the constraint that the distributions reduce to the PYTHIA distribution for $N_{\mathrm{part}} = 2$. The non-linear term accounted for the possible variation of the effective FCal acceptance resulting from an N_{part}-dependent backward rapidity shift of the produced soft particles with respect to the nucleon–nucleon frame [27]. The gamma distributions were summed

Table 1:
Average R_{coll} and $T_{p\mathrm{A}}$ values for the centrality intervals used in this analysis along with total systematic uncertainties. The R_{coll} values are with respect to 60–90% events, where $\langle N_{\mathrm{coll}} \rangle = 2.98^{+0.21}_{-0.29}$.

Centrality	R_{coll}	$T_{p\mathrm{A}}$ [mb^{-1}]
0–90%	-	$0.106^{+0.007}_{-0.006}$
60–90%	-	$0.043^{+0.003}_{-0.004}$
40–60%	$2.16^{+0.08}_{-0.07}$	$0.092^{+0.004}_{-0.006}$
30–40%	$3.00^{+0.21}_{-0.14}$	$0.126^{+0.003}_{-0.004}$
20–30%	$3.48^{+0.33}_{-0.18}$	$0.148^{+0.004}_{-0.002}$
10–20%	$4.05^{+0.49}_{-0.21}$	$0.172^{+0.007}_{-0.003}$
0–10%	$4.89^{+0.83}_{-0.27}$	$0.208^{+0.019}_{-0.005}$

over N_{part} with a $P(N_{\mathrm{part}})$ weighting to produce a hypothetical $\Sigma E_{\mathrm{T}}^{\mathrm{Pb}}$ distribution. That distribution was fit to the measured $\Sigma E_{\mathrm{T}}^{\mathrm{Pb}}$ distribution shown in Fig. 1 with the parameters of the extended WN model allowed to vary freely. The best fit, which contained a significant non-linear term, successfully described the $\Sigma E_{\mathrm{T}}^{\mathrm{Pb}}$ distribution in data over several orders of magnitude. From the results of the fit, the distribution of N_{part} values and the corresponding $\langle N_{\mathrm{part}} \rangle$ were calculated for each centrality interval. The resulting R_{coll} and $T_{p\mathrm{A}}$ values and corresponding systematic uncertainties, which are described in Section 8, are shown in Table 1.

5. Monte Carlo simulation

The performance of the jet reconstruction procedure was evaluated using a sample of 36 million events in which simulated $\sqrt{s} = 5.02$ TeV pp hard-scattering events were overlaid with minimum-bias p+Pb events recorded during the 2013 run. Thus the sample contains an underlying event (UE) contribution that is identical in all respects to the data. The simulated events were generated using PYTHIA [22] (version 6.425, AUET2B tune [24], CTEQ6L1 parton distribution functions [28]) and the detector effects were fully simulated using GEANT4 [29,30]. These events were produced for different p_{T} intervals of the generator-level ("truth") $R = 0.4$ jets. In total, the generator-level spectrum spans $10 < p_{\mathrm{T}} < 10^3$ GeV. Separate sets of 18 million events each were generated for the

4

two different beam directions to take into account any z-axis asymmetries in the detector. For each beam direction, the four-momenta of the generated particles were longitudinally boosted by a rapidity of ± 0.465 to match the corresponding beam conditions. The events were simulated using detector conditions appropriate to the two periods of the 2013 p+Pb run and reconstructed using the same algorithms as were applied to the experimental data. A separate 9-million-event sample of fully simulated 2.76 TeV PYTHIA pp hard scattering events (with the same version, tune and parton distribution function set) was used to evaluate the jet performance in $\sqrt{s} = 2.76$ TeV pp collisions during 2013 data-taking.

6. Jet reconstruction and performance

6.1. Reconstruction

The jet reconstruction and UE subtraction procedures were adapted from those used by ATLAS in Pb+Pb collisions, which are described in detail in Refs. [31,32], and are summarised in the following.

An iterative procedure was used to obtain an event-by-event estimate of the UE energy density while excluding contributions from jets to that estimate. To perform jet reconstruction, calorimeter cells were combined into towers with segmentation $\Delta\eta \times \Delta\phi = 0.1 \times 0.1$, and the anti-$k_t$ algorithm with $R = 0.2$ and $R = 0.4$ was applied to the towers. In addition, "track" jets were reconstructed by applying the anti-k_t algorithm with $R = 0.4$ to reconstructed tracks with $p_T > 0.5$ GeV.

A subset of the $R = 0.2$ jets were identified as "seed" jets and the cells within these jets were excluded from the background estimation. The average transverse energy density $\left\langle \frac{\mathrm{d}^2 E_T}{\mathrm{d}\eta \mathrm{d}\phi} \right\rangle$ in the remaining cells was then used as an estimate of the UE energy density. This estimate of the UE was constructed separately in each calorimeter layer and in $\Delta\eta = 0.1$ strips to accommodate the η-dependent variations in the UE activity present in p+Pb collisions.

The corrected energy in each cell, E_T^{sub}, was constructed by subtracting the estimate of the UE energy density from the original cell energy via $E_T^{\mathrm{sub}} = E_T - \left\langle \frac{\mathrm{d}^2 E_T}{\mathrm{d}\eta \mathrm{d}\phi} \right\rangle \Delta\eta \Delta\phi$ where E_T and $\Delta\eta \Delta\phi$ are the original transverse energy and area of the cell. For each tower included in a given jet, the energy of the cells in the tower was corrected with

this subtraction and the jet kinematics were recalculated. The updated jet kinematics were then used to determine a new set of seed jets and estimate of the UE energy density. All $R = 0.2$ calorimeter jets with $E_T > 4$ GeV and track jets with $p_T > 4$ GeV were identified as new seed jets, and a new estimate of $\left\langle \frac{\mathrm{d}^2 E_T}{\mathrm{d}\eta \mathrm{d}\phi} \right\rangle$ was performed excluding cells within $\Delta R < 0.4$ of the seed jet positions from the average.

After this second iteration step, the final set of $R = 0.4$ calorimeter jets used in the analysis was determined by updating their kinematics according to the latest UE estimate. The jet transverse energy and direction were reconstructed from the UE-subtracted energy in all cells contained in the jet, assuming these components to be massless. The mean subtracted UE transverse energy in p+Pb collisions was 2.4 GeV (1.4 GeV) for $R = 0.4$ jets with $|y^*| < 1$ ($y^* > 3$). In pp collisions, this procedure simply subtracts the UE pedestal deposited in the calorimeter which can arise, in part, from the presence of additional pp interactions in the same crossing (in-time pileup).

After this procedure, a small correction, typically a few percent, was applied to the transverse momentum of those jets which did not overlap with a region excluded from the background determination and thus were erroneously included in the initial estimate of the UE background. Then, the jet energies were corrected to account for the calorimeter energy response using an η- and p_T-dependent multiplicative factor that was derived from the simulations [33]. Following this calibration, a final multiplicative *in situ* calibration was applied to account for differences between the simulated detector response and data. The measured p_T of jets recoiling against objects with an independently calibrated energy scale – such as Z bosons, photons, or jets in a different region of the detector – was investigated. The *in situ* calibration, which typically differed from unity by a few percent, was derived by comparing this p_T balance in pp data with that in simulations in a fashion similar to that used previously within ATLAS [34].

6.2. Performance

The jet reconstruction performance was evaluated in the simulated samples by applying the same subtraction and reconstruction procedure as was applied to data. The resulting reconstructed jets with transverse momentum p_T^{reco} were compared

with their corresponding generator jets, which were produced by applying the anti-k_t algorithm to the final-state particles produced by PYTHIA, excluding muons and neutrinos. Each generator jet was matched to a reconstructed jet, and the p_T difference between the two jets was studied as a function of the generator jet transverse momentum, p_T^{gen}, and generator jet rapidity y^*, and in the six p+Pb event centrality intervals.

The reconstruction efficiency for jets having $p_T^{gen} > 25$ GeV was found to be greater than 99%. The performance was quantified by the means and standard deviations of the $\Delta p_T/p_T$ ($= p_T^{reco}/p_T^{gen} - 1$) distributions, referred to as the jet energy scale (JES) closure and jet energy resolution (JER) respectively. The JES closure in p+Pb events was less than 2% for $p_T^{gen} > 25$ GeV jets and was better than 1% for $p_T^{gen} > 100$ GeV jets. At low p_T^{gen}, the JES closure and JER exhibited a weak p+Pb centrality dependence, with differences in the JES closure of up to 1% and differences in the JER of up to 2% in the most central 0–10% events relative to the 60–90% peripheral events. In pp events, the JES closure was less than 1% in the entire kinematic range studied.

In order to quantify the degree of p_T-bin migration introduced by the detector response and reconstruction procedure, response matrices were populated by recording the p_T values of each generator–reconstructed jet pair. Separate matrices were constructed for each y^* interval and p+Pb centrality interval used in the analysis. The p_T bins used were chosen to increase with p_T such that the width of each bin was ≈ 0.25 of the bin low edge. Using this binning, the proportion of jets with reconstructed p_T in the same bin as their truth p_T monotonically increased with truth p_T and was 50–70%. The increased UE activity in central events relative to peripheral events led to a slightly larger resolution and energy scale non-closure for low-p_T jets in these events, resulting in larger bin-migration effects. At high jet p_T, where the role of the underlying event becomes less important than the intrinsic calorimetric jet energy resolution, the response was centrality independent within systematic uncertainties.

7. Data analysis

Jets in p+Pb collisions were selected by the minimum-bias triggers and jet triggers described in Section 2. Six jet triggers with different online jet-p_T thresholds were used for jets with $|\eta| < 3.2$

and one dedicated low-threshold trigger was used for jets with $|\eta| > 3.2$. The sampled luminosity (defined as the luminosity divided by the mean luminosity-weighted prescale) of the triggers increased with increasing p_T threshold. Offline jets were selected for the analysis by requiring a match to an online jet trigger. The efficiency of the various triggers was determined with respect to the minimum-bias trigger and to lower threshold jet triggers. For simplicity, each p_T bin used jets selected by only one jet trigger. In a given p_T bin, jets were selected by the lowest-threshold jet trigger for which the efficiency was determined to be greater than 99% in the bin. No additional corrections for the trigger efficiency were applied.

The double-differential per-event jet yields in p+Pb collisions were constructed via

$$\frac{1}{N_{evt}}\frac{d^2 N^{jet}}{dp_T dy^*} = \frac{1}{N_{evt}}\frac{N^{jet}}{\Delta p_T \Delta y^*}, \quad (3)$$

where N_{evt} is the total (unprescaled) number of MB p+Pb events sampled, N^{jet} is the yield of jets corrected for all detector effects and the instantaneous trigger prescale during data-taking, and Δp_T and Δy^* are the widths of the p_T and y^* bins. The centrality-dependent yields were constructed by restricting N_{evt} and N^{jet} to come from p+Pb events within a given centrality interval. The double-differential cross section in pp collisions was constructed via

$$\frac{d^2\sigma}{dp_T dy^*} = \frac{1}{L_{int}}\frac{N^{jet}}{\Delta p_T \Delta y^*}, \quad (4)$$

where L_{int} is the total integrated luminosity of the jet trigger used in the given p_T bin. The p_T binning in the pp cross-section was chosen such that the $x_T = 2p_T/\sqrt{s}$ binning between the p+Pb and pp datasets is the same.

Both the per-event yields in p+Pb collisions and the cross-section in pp collisions were restricted to the p_T range where the MC studies described in Section 6.2 show that the efficiency for a truth jet to remain in the same p_T bin is ≥ 50%. This p_T range was rapidity dependent, with the lowest p_T bin edge used ranging from 50 GeV in the most backward rapidity intervals studied to 25 GeV in the most forward intervals.

The measured p+Pb and pp yields were corrected for jet energy resolution and residual distortions of the jet energy scale which result in p_T-bin migration. For each rapidity interval, the yield was

corrected by the use of p_T-dependent (and, in the p+Pb case, centrality-dependent) bin-by-bin correction factors $C(p_T, y^*)$ obtained from the ratio of the reconstructed to the truth jet p_T distributions for jets originating in a true y^* bin, according to

$$C(p_T, y^*) = \frac{N_{\text{truth}}^{\text{jet}}(p_T, y^*)}{N_{\text{reco}}^{\text{jet}}(p_T, y^*)}, \qquad (5)$$

where $N_{\text{truth}}^{\text{jet}}$ ($N_{\text{reco}}^{\text{jet}}$) is the number of truth jets in the given p_T^{truth} (p_T^{reco}) bin in the corresponding MC samples.

Since the determination of the correction factors $C(p_T, y^*)$ is sensitive to the shape of the jet spectrum in the MC sample, the response matrices used to generate them were reweighted to provide a better match between the reconstructed distributions in data and simulated events. The spectrum of generator jets was weighted jet-by-jet by the ratio of the reconstructed spectrum in data to that in simulation. This ratio was found to be approximately linear in the logarithm of reconstructed p_T. A separate reweighting was performed for the p+Pb jet yield in each centrality interval, resulting in changes of $\leq 10\%$ from the original correction factors before reweighting. The resulting corrections to the p+Pb and pp yields were at most 30%, and were typically $\leq 10\%$ for jets with $p_T > 100$ GeV. These corrections were applied to the detector-level yield $N_{\text{reco}}^{\text{jet}}$ to give the particle-level yield via

$$N^{\text{jet}} = C(p_T, y^*)N_{\text{reco}}^{\text{jet}}. \qquad (6)$$

A $\sqrt{s} = 5.02$ TeV pp reference jet cross-section was constructed through the use of the corrected 2.76 TeV pp cross-section and a previous ATLAS measurement of the x_T-scaling between the inclusive jet cross-sections at $\sqrt{s} = 2.76$ TeV (measured using 0.20 pb^{-1} of data collected in 2011) and 7 TeV (measured using 37 pb^{-1} of data collected in 2010) [35]. In this previous analysis, the $\sqrt{s}$-scaled ratio ρ of the 2.76 TeV cross-section to that at 7 TeV was evaluated at fixed x_T,

$$\rho(x_T; y^*) = \left(\frac{2.76 \text{ TeV}}{7 \text{ TeV}}\right)^3 \frac{\mathrm{d}^2\sigma^{2.76 \text{ TeV}}/\mathrm{d}p_T\mathrm{d}y^*}{\mathrm{d}^2\sigma^{7 \text{ TeV}}/\mathrm{d}p_T\mathrm{d}y^*}, \qquad (7)$$

where $\mathrm{d}^2\sigma^{\sqrt{s}}/\mathrm{d}p_T\mathrm{d}y^*$ is the pp jet cross-section at the given centre-of-mass energy $\sqrt{s}$, and the numerator and denominator are each evaluated at the

same x_T (but different $p_T = x_T\sqrt{s}/2$). Equation (7) can be rearranged to define the cross-section at $\sqrt{s} = 7$ TeV in terms of that at 2.76 TeV times a multiplicative factor and divided by ρ.

The $\sqrt{s} = 5.02$ TeV pp cross-section at each p_T and y^* value was constructed by scaling the corrected $\sqrt{s} = 2.76$ TeV pp cross-section measured at the equivalent x_T according to

$$\frac{\mathrm{d}^2\sigma^{5.02 \text{ TeV}}}{\mathrm{d}p_T\mathrm{d}y^*}$$
$$= \rho(x_T; y^*)^{-0.643} \left(\frac{2.76 \text{ TeV}}{5.02 \text{ TeV}}\right)^3 \frac{\mathrm{d}^2\sigma^{2.76 \text{ TeV}}}{\mathrm{d}p_T\mathrm{d}y^*}, \qquad (8)$$

where the power $-\ln(2.76/5.02)/\ln(2.76/7) \approx -0.643$ interpolates between 2.76 TeV and 7 TeV to 5.02 TeV using a power-law collision energy dependence at each p_T and y^*. Since the jet energy scale and x_T interpolation uncertainties are large for the pp data at large rapidities ($|y^*| > 2.8$), a $\sqrt{s} = 5.02$ TeV reference is not constructed in that rapidity region.

The pp jet cross-section at $\sqrt{s} = 2.76$ TeV measured with the 2013 data was found to agree with the previous ATLAS measurement of the same quantity [35] within the systematic uncertainties.

8. Systematic uncertainties

The R_{CP} and $R_{p\text{Pb}}$ measurements are subject to systematic uncertainties arising from a number of sources: the jet energy scale (JES) and resolution (JER), differences in the spectral shape between data and simulation affecting the bin-by-bin correction factors, residual inefficiency in the trigger selection, and the estimates of the geometric quantities R_{coll} (in R_{CP}) and T_{pA} (in $R_{p\text{Pb}}$). In addition to these sources of uncertainty, which are common to the R_{CP} and $R_{p\text{Pb}}$ measurements, $R_{p\text{Pb}}$ is also subject to uncertainties from the x_T-interpolation of the $\sqrt{s} = 2.76$ TeV pp cross-section to the $\sqrt{s} = 5.02$ TeV centre-of-mass energy and from the integrated luminosity of the pp dataset.

Uncertainties in the JES and JER influence the correction of the p+Pb and pp jet spectra. The uncertainty in the JES was taken from studies of the *in situ* calorimeter response and systematic variations of the jet response in simulation [33], as well as studies of the relative energy scale difference between the jet reconstruction procedure in heavy-ion

collisions and the procedure used by ATLAS for inclusive jet measurements in 2.76 TeV and 7 TeV pp collisions [35,36]. The total JES uncertainty in the measured p_T range was $\lesssim 4\%$ for jets in $|y^*| < 2.8$, and $\lesssim 7\%$ for jets in $|y^*| > 2.8$. The sensitivity of the results to the uncertainty in the JES was evaluated separately for ten distinct sources of uncertainty. Each source was treated as fully uncorrelated with any other source, but fully correlated with itself in p_T, η, and $\sqrt{s}$. The uncertainty in the JER was taken from *in situ* studies of the dijet energy balance [37]. The JER uncertainty was generally $< 10\%$, except for low-p_T jets where it was $< 20\%$. The effects on the R_CP and $R_{p\mathrm{Pb}}$ measurements were evaluated through an additional smearing of the energy of reconstructed jets in the simulation such that the JER uncertainty was added to the original resolution in quadrature.

The resulting systematic uncertainties on R_CP (δR_CP) and $R_{p\mathrm{Pb}}$ ($\delta R_{p\mathrm{Pb}}$) were evaluated by producing new response matrices in accordance with each source of the JES uncertainty and the JER uncertainty, generating new correction factors, and calculating the new R_CP and $R_{p\mathrm{Pb}}$ results. Each JES and JER variation was applied to all rapidity bins and to both the p+Pb and pp response matrices simultaneously. The uncertainty on R_CP and $R_{p\mathrm{Pb}}$ from the total JES uncertainty was determined by adding the effects of the ten JES uncertainty sources in quadrature. Since the correction factors for the p+Pb spectra in different centrality intervals were affected to a similar degree by variations in the JES and JER, the effects tended to cancel in the R_CP ratio, and the resulting δR_CP were small. The resulting $\delta R_{p\mathrm{Pb}}$ values were somewhat larger than the δR_CP values due to the relative centre-of-mass shift between the p+Pb and pp collision systems. The centrality dependence of the JES and JER uncertainties in p+Pb events was negligible.

To achieve better correspondence with the data, the simulated jet spectrum was reweighted to match the spectral shape in data before deriving the bin-by-bin correction factors as described above. To determine the sensitivity of the results to this reweighting procedure, the slope of the fit to the ratio of the detector-level spectrum in data to that in simulation was varied by the fit uncertainty, and the correction factors were recomputed with this alternative weighting. The resulting $\delta R_{p\mathrm{Pb}}$ and δR_CP from the nominal values were included in the total systematic uncertainty.

As the jet triggers used for the data selection were evaluated to have greater than 99% efficiency in the p_T regions where they are used to select jets, an uncertainty of 1% was chosen for the centrality selected p+Pb yields and the pp cross-section in the range $20 < p_\mathrm{T} < 125$ GeV. This uncertainty was taken to be uncorrelated between the centrality-selected p+Pb yields and the pp cross-section, resulting in a 1.4% uncertainty on the R_CP and $R_{p\mathrm{Pb}}$ measurements.

The geometric quantities R_coll and T_pA and their uncertainties are listed in Table 1. These uncertainties arise from uncertainties in the geometric modelling of p+Pb collisions and in modelling the N_part dependence of the forward particle production measured by $\Sigma E_\mathrm{T}^\mathrm{Pb}$. In general, the uncertainties were asymmetric. Uncertainties in R_coll were largest for the ratio of the most central to the most peripheral interval (0–10%/60–90%), where they were $+17/-6\%$, and smallest in the 40–60%/60–90% ratio, where they were $+4/-3\%$. Uncertainties in T_pA were largest in the most central (0–10%) and most peripheral (60–90%) centrality intervals, where the upper or lower uncertainty was as high as 10%, and smaller for intervals in the middle of the p+Pb centrality range, where they reached a minimum of $+3/-2\%$ for the 20–30% interval.

The x_T-interpolation of the $\sqrt{s} = 2.76$ TeV pp jet cross-section to 5.02 TeV is sensitive to uncertainties in $\rho(x_\mathrm{T}, y^*)$, the $\sqrt{s}$-scaled ratio of jet spectra at 2.76 and 7 TeV. Following Eq. (8), the uncertainty in the interpolated pp cross-section ($\delta\sigma^{5.02~\mathrm{TeV}}$) at fixed x_T is related to the uncertainty in ρ ($\delta\rho$) via ($\delta\sigma^{5.02~\mathrm{TeV}}/\sigma^{5.02~\mathrm{TeV}}$) $= 0.643(\delta\rho/\rho)$, where $\delta\rho$ was taken from Ref. [35]. The values of $\delta\rho$ ranged from 5% to 23% in the region of the measurement and were generally larger at lower x_T and at larger rapidities.

The integrated luminosity for the 2013 pp dataset was determined by measuring the interaction rate with several ATLAS subdetectors. The absolute calibration was derived from three van der Meer scans [38] performed during the pp data-taking in 2013 in a fashion similar to that used previously within ATLAS [39] for pp data-taking at higher energies. The systematic uncertainty on the integrated luminosity was estimated to be 3.1%.

The uncertainties from the JES, JER, reweighting and x_T-interpolation are p_T and y^* dependent, while the uncertainties from the trigger, luminosity, and geometric factors are not. The total systematic uncertainty on the $R_{p\mathrm{Pb}}$ measurement ranges from
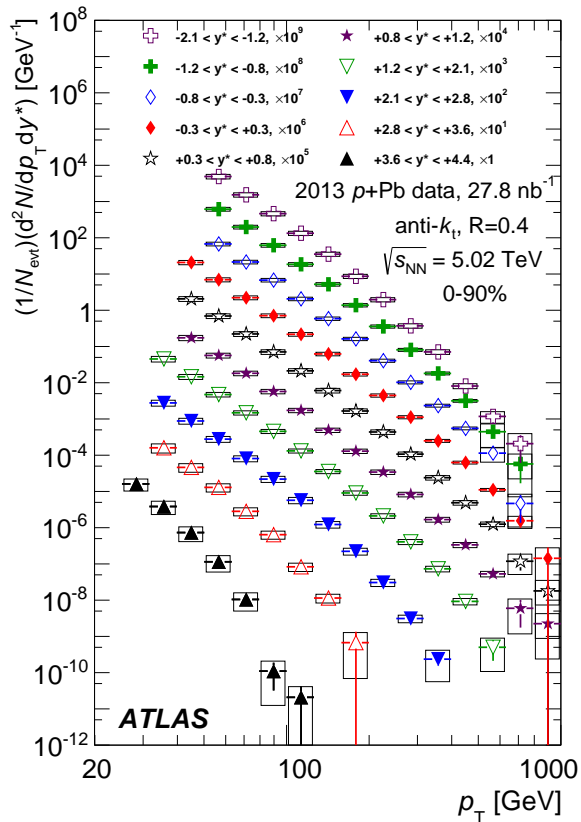
Fig. 2: Inclusive double-differential per-event jet yield in 0–90% p+Pb collisions as a function of jet p_T in different y^* bins. The yields are corrected for all detector effects. Vertical error bars represent the statistical uncertainty while the boxes represent the systematic uncertainties.

Fig. 3: Measured $R_{p\mathrm{Pb}}$ values for $R = 0.4$ jets in 0–90% p+Pb collisions. Each panel shows the jet $R_{p\mathrm{Pb}}$ in a different rapidity range. Vertical error bars represent the statistical uncertainty while the boxes represent the systematic uncertainties on the jet yields. The shaded box at the left edge of the $R_{p\mathrm{Pb}} = 1$ horizontal line indicates the systematic uncertainty on $T_{p\mathrm{A}}$ and the pp luminosity in quadrature. The shaded band represents a calculation using the EPS09 nuclear parton distribution function set.

7% at mid-rapidity and high p_T to 18% at forward rapidities and low p_T. In most p_T and rapidity bins, the dominant systematic uncertainty on $R_{p\mathrm{Pb}}$ is from the x_T-interpolation. The p_T- and y^*- dependent systematic uncertainties on R_{CP} are small. Near mid-rapidity or at high p_T, they are 2%, rising to approximately 12% at low p_T in forward rapidities. Thus, in most of the kinematic region studied, the dominant uncertainty on R_{CP} is from the geometric factors R_{coll}.

9. Results

Fig. 2 presents the fully corrected per-event jet yield as a function of p_T in 0–90% p+Pb collisions, for each of the jet centre-of-mass rapidity ranges used in this analysis. At mid-rapidity, the yields span over eight orders of magnitude.
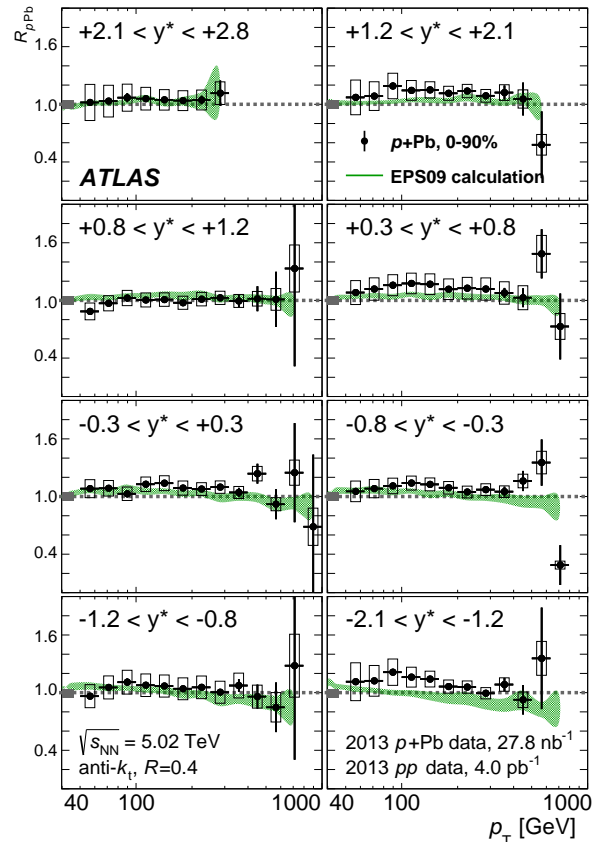
The jet nuclear modification factor $R_{p\mathrm{Pb}}$ for 0–90% p+Pb events is presented in Fig. 3 in the eight rapidity bins for which the pp reference was constructed. At most rapidities studied, the $R_{p\mathrm{Pb}}$ values show a slight ($\approx 10\%$) enhancement above one, although many bins are consistent with unity within the systematic uncertainties. At mid-rapidity, the $R_{p\mathrm{Pb}}$ values reach a maximum near 100 GeV. No large modification of the total yield of jets relative to the geometric expectation (under which $R_{p\mathrm{Pb}} = 1$) is observed. The data in Fig. 3 are compared to a next-to-leading order perturbative QCD calculation of $R_{p\mathrm{Pb}}$ with the EPS09 parameterisation of nuclear parton distribution functions [9], using CT10 [40] for the free proton parton
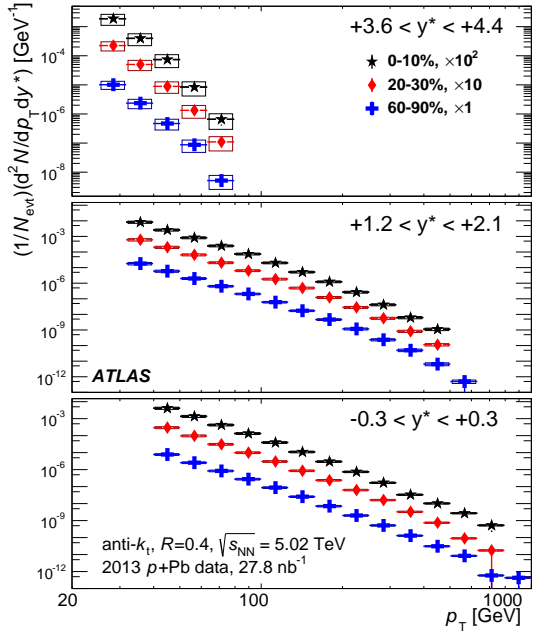
Fig. 4: Centrality-dependent inclusive double-differential per-event jet yield in p+Pb collisions, for three different rapidity ranges. Each panel shows the yield in central (stars), mid-central (diamonds) and peripheral (crosses) events. The yields are corrected for all detector effects. Vertical error bars represent the statistical uncertainty while the boxes represent the systematic uncertainties.

distribution functions and following the procedure for calculating jet production rates in p+Pb collisions described in Refs. [1,41]. The data are slightly higher than the calculation, but generally compatible with it within systematic uncertainties.

Fig. 4 shows examples of the centrality-selected p+Pb yields in three centrality intervals and three rapidity ranges.

The central-to-peripheral ratio R_{CP} for jets in p+Pb collisions is summarised in Fig. 5, where the R_{CP} values for three centrality intervals are shown in all rapidity ranges studied. The R_{CP} ratio shows a strong variation with centrality relative to the geometric expectation, under which $R_{\mathrm{CP}} = 1$. The jet R_{CP} for 0–10%/60–90% events is smaller than one at all rapidities for jet $p_{\mathrm{T}} > 100$ GeV and at all p_{T} at sufficiently forward (proton-going, $y^* > 0$) rapidities. Near mid-rapidity, the 40–60%/60–90% R_{CP} values are consistent with unity up to 100–200 GeV, but indicate a small suppression at higher p_{T}. In all rapidity intervals studied, R_{CP} decreases with increasing p_{T} and in increasingly more central collisions. Furthermore, at fixed p_{T}, R_{CP} decreases
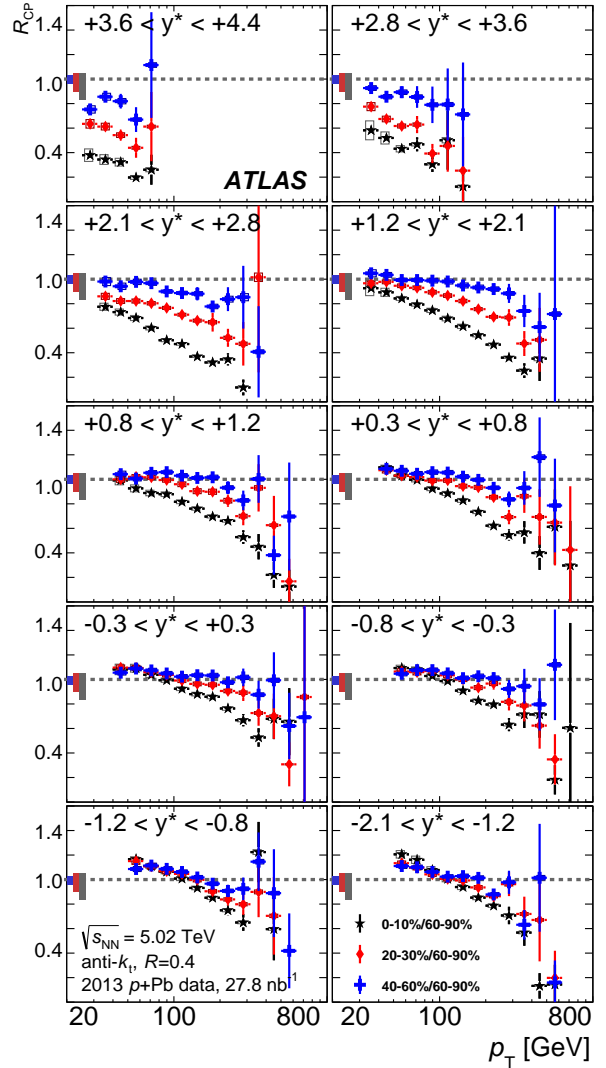

Fig. 5: Measured R_{CP} values for $R = 0.4$ jets in p+Pb collisions in central (stars), mid-central (diamonds) and mid-peripheral (crosses) events. Each panel shows the jet R_{CP} in a different rapidity range. Vertical error bars represent the statistical uncertainty while the boxes represent the systematic uncertainties on the jet yields. The shaded boxes at the left edge of the $R_{\mathrm{CP}} = 1$ horizontal line indicate the systematic uncertainty on R_{coll} for (from left to right) peripheral, mid-central and central events.

systematically at more forward rapidities. At the highest p_{T} in the most forward rapidity bin, the 0–10%/60–90% R_{CP} value is ≈ 0.2. In the backward rapidity direction (lead-going, $y^* < 0$), R_{CP} is found to be enhanced by 10–20% for low-p_{T} jets.

Fig. 6 summarises the jet $R_{p\mathrm{Pb}}$ in central, mid-central and peripheral events in all rapidity intervals studied. The patterns observed in the
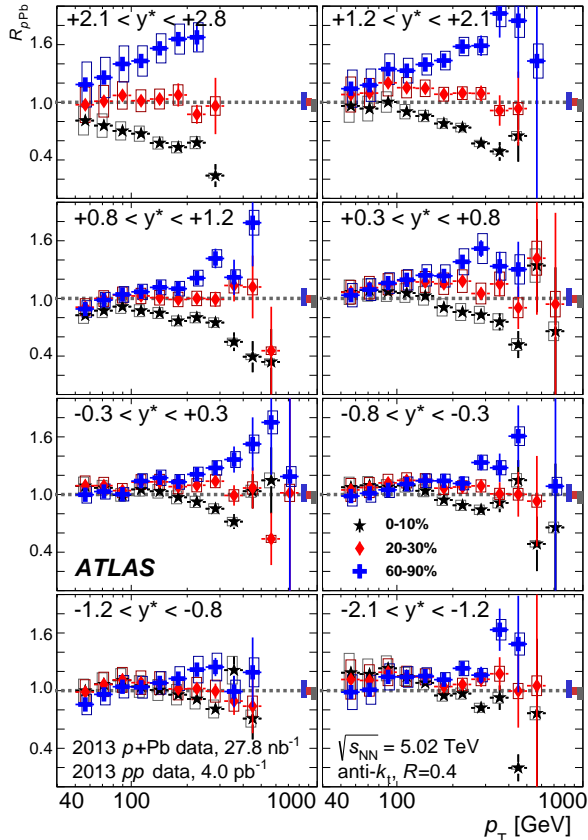
Fig. 6: Measured $R_{p\mathrm{Pb}}$ values for $R = 0.4$ jets in p+Pb collisions in central (stars), mid-central (diamonds) and peripheral (crosses) events. Each panel shows the jet $R_{p\mathrm{Pb}}$ in a different rapidity range. Vertical error bars represent the statistical uncertainty while the boxes represent the systematic uncertainties on the jet yields. The shaded boxes at the right edge of the $R_{p\mathrm{Pb}} = 1$ horizontal line indicate the systematic uncertainties on T_{pA} and the pp luminosity added in quadrature for (from left to right) peripheral, mid-central and central events.

centrality-dependent $R_{p\mathrm{Pb}}$ values are a consequence of the near-geometric scaling of the minimum bias $R_{p\mathrm{Pb}}$ values along with the strong modifications of the central-to-peripheral ratio R_{CP}. At sufficiently high p_{T}, $R_{p\mathrm{Pb}}$ in central events is found to be suppressed ($R_{p\mathrm{Pb}} < 1$) and in peripheral events to be enhanced ($R_{p\mathrm{Pb}} > 1$). Generally, these respective deviations from the geometric expectation (under which $R_{p\mathrm{Pb}} = 1$ for all centrality intervals) increase with p_{T} and, at fixed p_{T}, increase as the rapidity becomes more forward. Thus, the large effects in R_{CP} are consistent with a combination of modifications that have opposite sign in the centrality-dependent $R_{p\mathrm{Pb}}$ values but have little effect on the centrality-

inclusive (0–90%) $R_{p\mathrm{Pb}}$ values. At backward-going rapidities ($y^* < 0$) the $R_{p\mathrm{Pb}}$ value for low-p_{T} jets in all centrality intervals is consistent with unity within the uncertainties.

Given the observed suppression pattern as a function of jet rapidity, in which the suppression in R_{CP} at fixed p_{T} systematically increases at more forward-going rapidities, it is natural to ask if it is possible to find a single relationship between the R_{CP} values in the different rapidity intervals which is a function of jet kinematics alone. To test this, the R_{CP} values in each rapidity bin were plotted against the quantity $p_{\mathrm{T}} \times \cosh(\langle y^* \rangle) \approx p$, where $\langle y^* \rangle$ is the centre of the rapidity bin, and p is therefore approximately the total energy of the jet. The 0–10%/60–90% R_{CP} versus $p_{\mathrm{T}} \times \cosh(\langle y^* \rangle)$ is shown for all ten rapidity ranges in Fig. 7. When plotted against this variable, the R_{CP} values in each of the five forward-going rapidities ($y^* > +0.8$) fall along the same curve, which is approximately linear in the logarithm of p. This trend is also observed in the two most forward of the remaining rapidity intervals ($-0.3 < y^* < +0.8$), but the R_{CP} values at backward rapidities ($y^* < -0.3$) do not follow this trend. This pattern is also observed in other centrality intervals, albeit with a different slope in $\ln(p)$ for each centrality interval.

These patterns suggest that the observed modifications may depend on the initial parton kinematics, such as the longitudinal momentum fraction of the parton originating in the proton, x_p. In particular, a dependence on x_p would explain why the data follow a consistent trend vs. $p_{\mathrm{T}} \times \cosh(\langle y^* \rangle)$ at forward rapidities (where jet production at a given jet energy p is dominated by $x_p \sim p/(\sqrt{s}/2)$ partons in the proton) but do not do so at backward rapidities (where the longitudinal momentum fraction of the parton originating in the lead nucleus, x_{Pb}, as well as x_p are both needed to relate the jet and parton kinematics).

By analogy with Fig. 7 where the R_{CP} values are plotted versus $p_{\mathrm{T}} \times \cosh(\langle y^* \rangle)$, the $R_{p\mathrm{Pb}}$ values in the four most forward-going bins studied are plotted against this variable in Fig. 8. The $R_{p\mathrm{Pb}}$ values in central and peripheral events are shown separately. Although the systematic uncertainties are larger on $R_{p\mathrm{Pb}}$ than on R_{CP}, the observed behaviour for jets with $p_{\mathrm{T}} > 150$ GeV is consistent with the nuclear modifications depending only on the approximate total jet energy $p_{\mathrm{T}} \times \cosh(\langle y^* \rangle)$. In central (peripheral) events, the $R_{p\mathrm{Pb}}$ values at forward rapidities are consistent
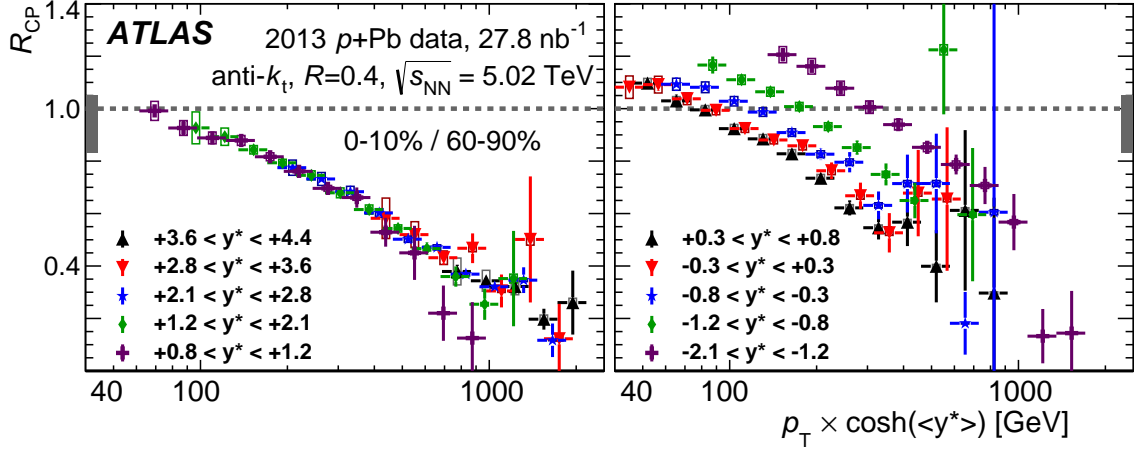
11

Fig. 7: Measured R_{CP} values for $R = 0.4$ jets in 0–10% p+Pb collisions. The panel on the left shows the five rapidity ranges that are the most forward-going, while the panel on the right shows the remaining five. The R_{CP} values at each rapidity are plotted as a function of $p_{\mathrm{T}} \times \cosh(\langle y^* \rangle)$, where $\langle y^* \rangle$ is the midpoint of the rapidity bin. Vertical error bars represent the statistical uncertainty while the boxes represent the systematic uncertainties on the jet yields. The shaded box at the left edge (in the left panel) and right edge (in the right panel) of the $R_{\mathrm{CP}} = 1$ horizontal line indicates the systematic uncertainty on R_{coll}.
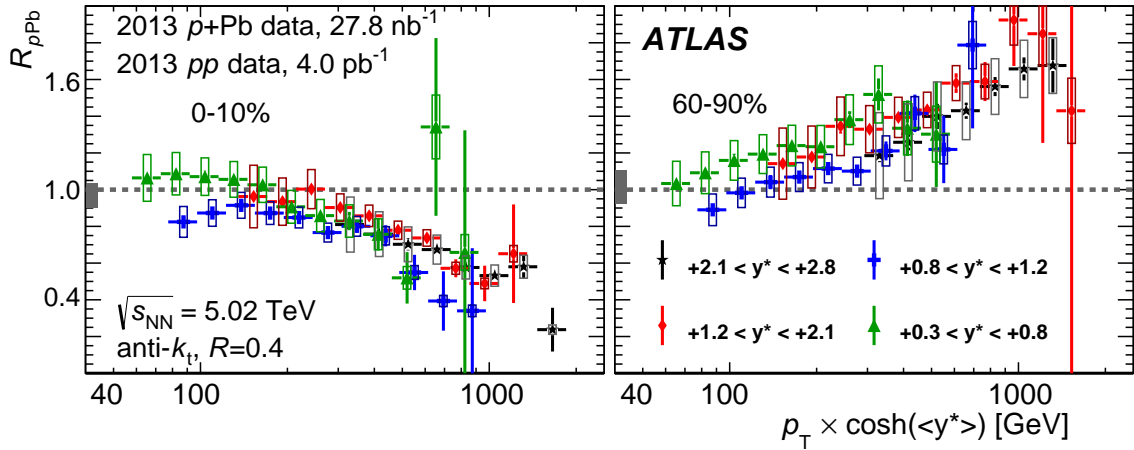

Fig. 8: Measured $R_{p\mathrm{Pb}}$ values for $R = 0.4$ jets in p+Pb collisions displayed for multiple rapidity ranges, showing 0–10% events in the left panel and 60–90% events in the right panel. The $R_{p\mathrm{Pb}}$ at each rapidity is plotted as a function of $p_{\mathrm{T}} \times \cosh(\langle y^* \rangle)$, where $\langle y^* \rangle$ is the midpoint of the rapidity bin. Vertical error bars represent the statistical uncertainty while the boxes represent the systematic uncertainties on the jet yields. The shaded box at the left edge of the $R_{p\mathrm{Pb}} = 1$ horizontal line indicates the systematic uncertainties on T_{pA} and the pp luminosity added in quadrature.

with a rapidity-independent decreasing (increasing) function of $p_{\mathrm{T}} \times \cosh(\langle y^* \rangle)$. Thus, the single trend in R_{CP} versus $p_{\mathrm{T}} \times \cosh(\langle y^* \rangle)$ at forward rapidities appears to arise from opposite trends in the central and peripheral $R_{p\mathrm{Pb}}$, both a single function of $p_{\mathrm{T}} \times \cosh(\langle y^* \rangle)$.

The results presented here use the standard Glauber model with fixed σ_{NN} to estimate the geometric quantities. The impact of geometric mod-els which incorporate event-by-event changes in the configuration of the proton wavefunction [42] has also been studied. Using the so called Glauber–Gribov Colour Fluctuation model to determine the geometric parameters amplifies the effects seen with the Glauber model. In this model, the suppression in central events and the enhancement in peripheral events would be increased.

10. Conclusions

This paper presents the results of a measurement of the centrality dependence of jet production in p+Pb collisions at $\sqrt{s_{NN}} = 5.02$ TeV over a wide kinematic range. The data were collected with the ATLAS detector at the LHC and corresponds to 27.8 nb^{-1} of integrated luminosity. The centrality of p+Pb collisions was characterised using the total transverse energy measured in the forward calorimeter on the Pb-going side covering the interval $-4.9 < \eta < -3.2$. The average number of nucleon–nucleon collisions and the mean nuclear thickness factor were evaluated for each centrality interval using a Glauber Monte Carlo analysis.

Results are presented for the nuclear modification factor $R_{p\mathrm{Pb}}$ with respect to a measurement of the inclusive jet cross-section in $\sqrt{s} = 2.76$ TeV pp collisions corresponding to 4.0 pb^{-1} of integrated luminosity. The pp cross-section was x_{T}-interpolated to 5.02 TeV using previous ATLAS measurements of inclusive jet production at 2.76 and 7 TeV. Results are also shown for the central-to-peripheral ratio R_{CP}. The centrality-inclusive $R_{p\mathrm{Pb}}$ results for 0–90% collisions indicate only a modest enhancement over the geometric expectation. This enhancement has a weak p_{T} and rapidity dependence and is generally consistent with predictions from the modification of the parton distribution functions in the nucleus, which is small in the kinematic region probed by this measurement.

The results of the R_{CP} measurement indicate a strong centrality-dependent reduction in the yield of jets in central collisions relative to that in peripheral collisions, after accounting for the effects of the collision geometries. In addition, the reduction becomes more pronounced with increasing jet p_{T} and at more forward (downstream proton) rapidities. These two results are reconciled by the centrality-dependent $R_{p\mathrm{Pb}}$ results, which show a suppression in central collisions and enhancement in peripheral collisions, a pattern which is systematic in p_{T} and y^*.

The R_{CP} and $R_{p\mathrm{Pb}}$ measurements at forward rapidities are also reported as a function of $p_{\mathrm{T}} \times \cosh(\langle y^* \rangle)$, the approximate total jet energy. When plotted this way, the results from different rapidity intervals follow a similar trend. This suggests that the mechanism responsible for the observed effects may depend only on the total jet energy or, more generally, on the underlying parton–parton kinematics such as the fractional longitudinal momentum of the parton originating in the proton.

If the relationship between the centrality intervals and proton–lead collision impact parameter determined by the geometric models is correct, these results imply large, impact parameter-dependent changes in the number of partons available for hard scattering. However, they may also be the result of a correlation between the kinematics of the scattering and the soft interactions resulting in particle production at backward (Pb-going) rapidities [43,44].

Recently, the effects observed here have been hypothesized as arising from a suppression of the soft particle multiplicity in collisions producing high energy jets [45]. Independently, it has also been argued that proton configurations containing a large-x parton interact with nucleons in the nucleus with a reduced cross-section, resulting in the observed modifications [46]. In any case the presence of such correlations would challenge the usual factorisation-based framework for describing hard scattering processes in collisions involving nuclei.

References

[1] C. Salgado, et al., J. Phys. G 39 (2012) 015010. arXiv:1105.3919.

[2] I. Arsene, et al., Phys. Rev. Lett. 93 (2004) 242303. arXiv:nucl-ex/0403005.

[3] S. S. Adler, et al., Phys. Rev. Lett. 94 (2005) 082302. arXiv:nucl-ex/0411054.

[4] J. Adams, et al., Phys. Rev. Lett. 97 (2006) 152302. arXiv:nucl-ex/0602011.

[5] A. Adare, et al., Phys. Rev. Lett. 107 (2011) 172301. arXiv:1105.5112.

[6] J. Jalilian-Marian, Y. V. Kovchegov, Prog. Part. Nucl. Phys. 56 (2006) 104. arXiv:hep-ph/0505052.

[7] F. Gelis, E. Iancu, J. Jalilian-Marian, R. Venugopalan, Ann. Rev. Nucl. Part. Sci. 60 (2010) 463. arXiv:1002.0333.

[8] D. Kharzeev, Y. Kovchegov, K. Tuchin, Phys. Lett. B 599 (2004) 23. arXiv:hep-ph/0405045.

[9] K. Eskola, H. Paukkunen, C. Salgado, J. High Energy Phys. 0904 (2009) 065. arXiv:0902.4154.

[10] B. Kopeliovich, et al., Phys. Rev. C 72 (2005) 054606. arXiv:hep-ph/0501260.

[11] J.-W. Qiu, I. Vitev, Phys. Lett. B 632 (2006) 507. arXiv:hep-ph/0405068.

[12] M. Cacciari, G. P. Salam, G. Soyez, J. High Energy Phys. 0804 (2008) 063. arXiv:0802.1189.

[13] S. S. Adler, et al., Phys. Rev. Lett. 98 (2007) 172302. arXiv:nucl-ex/0610036.

[14] B. B. Back, et al., Phys. Rev. C 70 (2004) 061901. arXiv:nucl-ex/0406017.

[15] M. L. Miller, K. Reygers, S. J. Sanders, P. Steinberg, Ann. Rev. Nucl. Part. Sci. 57 (2007) 205. arXiv:nucl-ex/0701025.

[16] ATLAS Collaboration, JINST 3 (2008) S08003.

[17] ATLAS Collaboration, Eur. Phys. J. C 70 (2010) 787. arXiv:1004.5293.

[18] ATLAS Collaboration, Eur. Phys. J. C 72 (2012) 1849. arXiv:1110.1530.

[19] ATLAS Collaboration, New J. Phys. 13 (2010) 053033. arXiv:1012.5104.

[20] ATLAS Collaboration, Phys. Lett. B 710 (2012) 363. arXiv:1108.6027.

[21] B. Alver, M. Baker, C. Loizides, P. Steinberg, The PHOBOS Glauber Monte Carlo, arXiv:0805.4411.

[22] T. Sjostrand, S. Mrenna, P. Z. Skands, J. High Energy Phys. 0605 (2006) 026. arXiv:hep-ph/0603175.

[23] T. Sjostrand, S. Mrenna, P. Z. Skands, Comput. Phys. Commun. 178 (2008) 852. arXiv:0710.3820.

[24] ATLAS Collaboration, ATL-PHYS-PUB-2012-003 http://cds.cern.ch/record/1474107.

[25] A. Martin, W. Stirling, R. Thorne, G. Watt, Eur. Phys. J. C 63 (2009) 189. arXiv:0901.0002.

[26] A. Bialas, M. Bleszynski, W. Czyz, Nucl. Phys. B 111 (1976) 461.

[27] P. Steinberg, Inclusive pseudorapidity distributions in $p(d)$+A collisions modeled with shifted rapidity distributions, arXiv:nucl-ex/0703002.

[28] J. Pumplin, et al., J. High Energy Phys. 0207 (2002) 012. arXiv:hep-ph/0201195.

[29] GEANT4 Collaboration, S. Agostinelli, et al., Nucl. Instrum. Meth. A 506 (2003) 250.

[30] ATLAS Collaboration, Eur. Phys. J. C 70 (2010) 823. arXiv:1005.4568.

[31] ATLAS Collaboration, Phys. Lett. B 719 (2013) 220. arXiv:1208.1967.

[32] ATLAS Collaboration, Phys. Rev. Lett. 111 (2013) 152301. arXiv:1306.6469.

[33] ATLAS Collaboration, Eur. Phys. J. C 73 (2013) 2304. arXiv:1112.6426.

[34] ATLAS Collaboration, Jet energy measurement and its systematic uncertainty in proton-proton collisions at $\sqrt{s}$ = 7 TeV with the ATLAS detector, arXiv:1406.0076.

[35] ATLAS Collaboration, Eur. Phys. J. C 73 (2013) 2509. arXiv:1304.4739.

[36] ATLAS Collaboration, Phys. Rev. D 86 (2012) 014022. arXiv:1112.6297.

[37] ATLAS Collaboration, Eur. Phys. J. C 73 (2013) 2306. arXiv:1210.6210.

[38] S. van der Meer, CERN-ISR-PO-68-31 http://cds.cern.ch/record/296752/.

[39] ATLAS Collaboration, Eur. Phys. J. C 73 (2013) 2518. arXiv:1302.4393.

[40] H.-L. Lai, M. Guzzi, J. Huston, Z. Li, P. M. Nadolsky, et al., Phys. Rev. D 82 (2010) 074024. arXiv:1007.2241.

[41] J. Albacete, N. Armesto, R. Baier, G. Barnafoldi, J. Barrette, et al., Int. J. Mod. Phys. E 22 (2013) 1330007. arXiv:1301.3395.

[42] M. Alvioli, M. Strikman, Phys. Lett. B 722 (2013) 347. arXiv:1301.0728.

[43] M. Alvioli, L. Frankfurt, V. Guzey, M. Strikman, Phys. Rev. C 90 (2014) 034914. arXiv:1402.2868.

[44] C. E. Coleman-Smith, B. Müller, Phys. Rev. D 89 (2014) 025019. arXiv:1307.5911.

[45] A. Bzdak, V. Skokov, S. Bathe, Centrality dependence of high energy jets in p+Pb collisions at the LHC. arXiv:1408.3156.

[46] M. Alvioli, B. Cole, L. Frankfurt, M. Strikman, Evidence for x-dependent proton color fluctuations in pA collisions at the LHC. arXiv:1409.7381.

14

The ATLAS Collaboration

G. Aad[84], B. Abbott[112], J. Abdallah[152], S. Abdel Khalek[116], O. Abdinov[11], R. Aben[106], B. Abi[113],
M. Abolins[89], O.S. AbouZeid[159], H. Abramowicz[154], H. Abreu[153], R. Abreu[30], Y. Abulaiti[147a,147b],
B.S. Acharya[165a,165b,a], L. Adamczyk[38a], D.L. Adams[25], J. Adelman[177], S. Adomeit[99], T. Adye[130],
T. Agatonovic-Jovin[13a], J.A. Aguilar-Saavedra[125a,125f], M. Agustoni[17], S.P. Ahlen[22], F. Ahmadov[64,b],
G. Aielli[134a,134b], H. Akerstedt[147a,147b], T.P.A. Åkesson[80], G. Akimoto[156], A.V. Akimov[95],
G.L. Alberghi[20a,20b], J. Albert[170], S. Albrand[55], M.J. Alconada Verzini[70], M. Aleksa[30], I.N. Aleksandrov[64],
C. Alexa[26a], G. Alexander[154], G. Alexandre[49], T. Alexopoulos[10], M. Alhroob[165a,165c], G. Alimonti[90a],
L. Alio[84], J. Alison[31], B.M.M. Allbrooke[18], L.J. Allison[71], P.P. Allport[73], J. Almond[83], A. Aloisio[103a,103b],
A. Alonso[36], F. Alonso[70], C. Alpigiani[75], A. Altheimer[35], B. Alvarez Gonzalez[89], M.G. Alviggi[103a,103b],
K. Amako[65], Y. Amaral Coutinho[24a], C. Amelung[23], D. Amidei[88], S.P. Amor Dos Santos[125a,125c],
A. Amorim[125a,125b], S. Amoroso[48], N. Amram[154], G. Amundsen[23], C. Anastopoulos[140], L.S. Ancu[49],
N. Andari[30], T. Andeen[35], C.F. Anders[58b], G. Anders[30], K.J. Anderson[31], A. Andreazza[90a,90b],
V. Andrei[58a], X.S. Anduaga[70], S. Angelidakis[9], I. Angelozzi[106], P. Anger[44], A. Angerami[35],
F. Anghinolfi[30], A.V. Anisenkov[108,c], N. Anjos[125a], A. Annovi[47], A. Antonaki[9], M. Antonelli[47],
A. Antonov[97], J. Antos[145b], F. Anulli[133a], M. Aoki[65], L. Aperio Bella[18], R. Apolle[119,d], G. Arabidze[89],
I. Aracena[144], Y. Arai[65], J.P. Araque[125a], A.T.H. Arce[45], J-F. Arguin[94], S. Argyropoulos[42], M. Arik[19a],
A.J. Armbruster[30], O. Arnaez[30], V. Arnal[81], H. Arnold[48], M. Arratia[28], O. Arslan[21], A. Artamonov[96],
G. Artoni[23], S. Asai[156], N. Asbah[42], A. Ashkenazi[154], B. Åsman[147a,147b], L. Asquith[6], K. Assamagan[25],
R. Astalos[145a], M. Atkinson[166], N.B. Atlay[142], B. Auerbach[6], K. Augsten[127], M. Aurousseau[146b],
G. Avolio[30], G. Azuelos[94,e], Y. Azuma[156], M.A. Baak[30], A.E. Baas[58a], C. Bacci[135a,135b], H. Bachacou[137],
K. Bachas[155], M. Backes[30], M. Backhaus[30], J. Backus Mayes[144], E. Badescu[26a], P. Bagiacchi[133a,133b],
P. Bagnaia[133a,133b], Y. Bai[33a], T. Bain[35], J.T. Baines[130], O.K. Baker[177], P. Balek[128], F. Balli[137],
E. Banas[39], Sw. Banerjee[174], A.A.E. Bannoura[176], V. Bansal[170], H.S. Bansil[18], L. Barak[173],
S.P. Baranov[95], E.L. Barberio[87], D. Barberis[50a,50b], M. Barbero[84], T. Barillari[100], M. Barisonzi[176],
T. Barklow[144], N. Barlow[28], B.M. Barnett[130], R.M. Barnett[15], Z. Barnovska[5], A. Baroncelli[135a],
G. Barone[49], A.J. Barr[119], F. Barreiro[81], J. Barreiro Guimarães da Costa[57], R. Bartoldus[144],
A.E. Barton[71], P. Bartos[145a], V. Bartsch[150], A. Bassalat[116], A. Basye[166], R.L. Bates[53], J.R. Batley[28],
M. Battaglia[138], M. Battistin[30], F. Bauer[137], H.S. Bawa[144,f], M.D. Beattie[71], T. Beau[79],
P.H. Beauchemin[162], R. Beccherle[123a,123b], P. Bechtle[21], H.P. Beck[17,g], K. Becker[176], S. Becker[99],
M. Beckingham[171], C. Becot[116], A.J. Beddall[19c], A. Beddall[19c], S. Bedikian[177], V.A. Bednyakov[64],
C.P. Bee[149], L.J. Beemster[106], T.A. Beermann[176], M. Begel[25], K. Behr[119], C. Belanger-Champagne[86],
P.J. Bell[49], W.H. Bell[49], G. Bella[154], L. Bellagamba[20a], A. Bellerive[29], M. Bellomo[85], K. Belotskiy[97],
O. Beltramello[30], O. Benary[154], D. Benchekroun[136a], K. Bendtz[147a,147b], N. Benekos[166],
Y. Benhammou[154], E. Benhar Noccioli[49], J.A. Benitez Garcia[160b], D.P. Benjamin[45], J.R. Bensinger[23],
K. Benslama[131], S. Bentvelsen[106], D. Berge[106], E. Bergeaas Kuutmann[167], N. Berger[5], F. Berghaus[170],
J. Beringer[15], C. Bernard[22], P. Bernat[77], C. Bernius[78], F.U. Bernlochner[170], T. Berry[76], P. Berta[128],
C. Bertella[84], G. Bertoli[147a,147b], F. Bertolucci[123a,123b], C. Bertsche[112], D. Bertsche[112], M.I. Besana[90a],
G.J. Besjes[105], O. Bessidskaia[147a,147b], M. Bessner[42], N. Besson[137], C. Betancourt[48], S. Bethke[100],
W. Bhimji[46], R.M. Bianchi[124], L. Bianchini[23], M. Bianco[30], O. Biebel[99], S.P. Bieniek[77], K. Bierwagen[54],
J. Biesiada[15], M. Biglietti[135a], J. Bilbao De Mendizabal[49], H. Bilokon[47], M. Bindi[54], S. Binet[116],
A. Bingul[19c], C. Bini[133a,133b], C.W. Black[151], J.E. Black[144], K.M. Black[22], D. Blackburn[139], R.E. Blair[6],
J.-B. Blanchard[137], T. Blazek[145a], I. Bloch[42], C. Blocker[23], W. Blum[82,*], U. Blumenschein[54],
G.J. Bobbink[106], V.S. Bobrovnikov[108,c], S.S. Bocchetta[80], A. Bocci[45], C. Bock[99], C.R. Boddy[119],
M. Boehler[48], T.T. Boek[176], J.A. Bogaerts[30], A.G. Bogdanchikov[108], A. Bogouch[91,*], C. Bohm[147a],
J. Bohm[126], V. Boisvert[76], T. Bold[38a], V. Boldea[26a], A.S. Boldyrev[98], M. Bomben[79], M. Bona[75],
M. Boonekamp[137], A. Borisov[129], G. Borissov[71], M. Borri[83], S. Borroni[42], J. Bortfeldt[99],
V. Bortolotto[135a,135b], K. Bos[106], D. Boscherini[20a], M. Bosman[12], H. Boterenbrood[106], J. Boudreau[124],
J. Bouffard[2], E.V. Bouhova-Thacker[71], D. Boumediene[34], C. Bourdarios[116], N. Bousson[113],
S. Boutouil[136d], A. Boveia[31], J. Boyd[30], I.R. Boyko[64], J. Bracinik[18], A. Brandt[8], G. Brandt[15],
O. Brandt[58a], U. Bratzler[157], B. Brau[85], J.E. Brau[115], H.M. Braun[176,*], S.F. Brazzale[165a,165c],

B. Brelier[159], K. Brendlinger[121], A.J. Brennan[87], R. Brenner[167], S. Bressler[173], K. Bristow[146c],
T.M. Bristow[46], D. Britton[53], F.M. Brochu[28], I. Brock[21], R. Brock[89], C. Bromberg[89], J. Bronner[100],
G. Brooijmans[35], T. Brooks[76], W.K. Brooks[32b], J. Brosamer[15], E. Brost[115], J. Brown[55],
P.A. Bruckman de Renstrom[39], D. Bruncko[145b], R. Bruneliere[48], S. Brunet[60], A. Bruni[20a], G. Bruni[20a],
M. Bruschi[20a], L. Bryngemark[80], T. Buanes[14], Q. Buat[143], F. Bucci[49], P. Buchholz[142],
R.M. Buckingham[119], A.G. Buckley[53], S.I. Buda[26a], I.A. Budagov[64], F. Buehrer[48], L. Bugge[118],
M.K. Bugge[118], O. Bulekov[97], A.C. Bundock[73], H. Burckhart[30], S. Burdin[73], B. Burghgrave[107],
S. Burke[130], I. Burmeister[43], E. Busato[34], D. Büscher[48], V. Büscher[82], P. Bussey[53], C.P. Buszello[167],
B. Butler[57], J.M. Butler[22], A.I. Butt[3], C.M. Buttar[53], J.M. Butterworth[77], P. Butti[106], W. Buttinger[28],
A. Buzatu[53], M. Byszewski[10], S. Cabrera Urbán[168], D. Caforio[20a,20b], O. Cakir[4a], P. Calafiura[15],
A. Calandri[137], G. Calderini[79], P. Calfayan[99], R. Calkins[107], L.P. Caloba[24a], D. Calvet[34], S. Calvet[34],
R. Camacho Toro[49], S. Camarda[42], D. Cameron[118], L.M. Caminada[15], R. Caminal Armadans[12],
S. Campana[30], M. Campanelli[77], A. Campoverde[149], V. Canale[103a,103b], A. Canepa[160a], M. Cano Bret[75],
J. Cantero[81], R. Cantrill[125a], T. Cao[40], M.D.M. Capeans Garrido[30], I. Caprini[26a], M. Caprini[26a],
M. Capua[37a,37b], R. Caputo[82], R. Cardarelli[134a], T. Carli[30], G. Carlino[103a], L. Carminati[90a,90b],
S. Caron[105], E. Carquin[32a], G.D. Carrillo-Montoya[146c], J.R. Carter[28], J. Carvalho[125a,125c], D. Casadei[77],
M.P. Casado[12], M. Casolino[12], E. Castaneda-Miranda[146b], A. Castelli[106], V. Castillo Gimenez[168],
N.F. Castro[125a], P. Catastini[57], A. Catinaccio[30], J.R. Catmore[118], A. Cattai[30], G. Cattani[134a,134b],
J. Caudron[82], S. Caughron[89], V. Cavaliere[166], D. Cavalli[90a], M. Cavalli-Sforza[12], V. Cavasinni[123a,123b],
F. Ceradini[135a,135b], B.C. Cerio[45], K. Cerny[128], A.S. Cerqueira[24b], A. Cerri[150], L. Cerrito[75], F. Cerutti[15],
M. Cerv[30], A. Cervelli[17], S.A. Cetin[19b], A. Chafaq[136a], D. Chakraborty[107], I. Chalupkova[128], P. Chang[166],
B. Chapleau[86], J.D. Chapman[28], D. Charfeddine[116], D.G. Charlton[18], C.C. Chau[159],
C.A. Chavez Barajas[150], S. Cheatham[86], A. Chegwidden[89], S. Chekanov[6], S.V. Chekulaev[160a],
G.A. Chelkov[64,h], M.A. Chelstowska[88], C. Chen[63], H. Chen[25], K. Chen[149], L. Chen[33d,i], S. Chen[33c],
X. Chen[146c], Y. Chen[66], Y. Chen[35], H.C. Cheng[88], Y. Cheng[31], A. Cheplakov[64],
R. Cherkaoui El Moursli[136e], V. Chernyatin[25,*], E. Cheu[7], L. Chevalier[137], V. Chiarella[47],
G. Chiefari[103a,103b], J.T. Childers[6], A. Chilingarov[71], G. Chiodini[72a], A.S. Chisholm[18], R.T. Chislett[77],
A. Chitan[26a], M.V. Chizhov[64], S. Chouridou[9], B.K.B. Chow[99], D. Chromek-Burckhart[30], M.L. Chu[152],
J. Chudoba[126], J.J. Chwastowski[39], L. Chytka[114], G. Ciapetti[133a,133b], A.K. Ciftci[4a], R. Ciftci[4a],
D. Cinca[53], V. Cindro[74], A. Ciocio[15], P. Cirkovic[13b], Z.H. Citron[173], M. Citterio[90a], M. Ciubancan[26a],
A. Clark[49], P.J. Clark[46], R.N. Clarke[15], W. Cleland[124], J.C. Clemens[84], C. Clement[147a,147b], Y. Coadou[84],
M. Cobal[165a,165c], A. Coccaro[139], J. Cochran[63], L. Coffey[23], J.G. Cogan[144], J. Coggeshall[166], B. Cole[35],
S. Cole[107], A.P. Colijn[106], J. Collot[55], T. Colombo[58c], G. Colon[85], G. Compostella[100],
P. Conde Muiño[125a,125b], E. Coniavitis[48], M.C. Conidi[12], S.H. Connell[146b], I.A. Connelly[76],
S.M. Consonni[90a,90b], V. Consorti[48], S. Constantinescu[26a], C. Conta[120a,120b], G. Conti[57], F. Conventi[103a,j],
M. Cooke[15], B.D. Cooper[77], A.M. Cooper-Sarkar[119], N.J. Cooper-Smith[76], K. Copic[15], T. Cornelissen[176],
M. Corradi[20a], F. Corriveau[86,k], A. Corso-Radu[164], A. Cortes-Gonzalez[12], G. Cortiana[100], G. Costa[90a],
M.J. Costa[168], D. Costanzo[140], D. Côté[8], G. Cottin[28], G. Cowan[76], B.E. Cox[83], K. Cranmer[109], G. Cree[29],
S. Crépé-Renaudin[55], F. Crescioli[79], W.A. Cribbs[147a,147b], M. Crispin Ortuzar[119], M. Cristinziani[21],
V. Croft[105], G. Crosetti[37a,37b], C.-M. Cuciuc[26a], T. Cuhadar Donszelmann[140], J. Cummings[177],
M. Curatolo[47], C. Cuthbert[151], H. Czirr[142], P. Czodrowski[3], Z. Czyczula[177], S. D'Auria[53], M. D'Onofrio[73],
M.J. Da Cunha Sargedas De Sousa[125a,125b], C. Da Via[83], W. Dabrowski[38a], A. Dafinca[119], T. Dai[88],
O. Dale[14], F. Dallaire[94], C. Dallapiccola[85], M. Dam[36], A.C. Daniells[18], M. Dano Hoffmann[137], V. Dao[48],
G. Darbo[50a], S. Darmora[8], J. Dassoulas[42], A. Dattagupta[60], W. Davey[21], C. David[170], T. Davidek[128],
E. Davies[119,d], M. Davies[154], O. Davignon[79], A.R. Davison[77], P. Davison[77], Y. Davygora[58a], E. Dawe[143],
I. Dawson[140], R.K. Daya-Ishmukhametova[85], K. De[8], R. de Asmundis[103a], S. De Castro[20a,20b],
S. De Cecco[79], N. De Groot[105], P. de Jong[106], H. De la Torre[81], F. De Lorenzi[63], L. De Nooij[106],
D. De Pedis[133a], A. De Salvo[133a], U. De Sanctis[165a,165b], A. De Santo[150], J.B. De Vivie De Regie[116],
W.J. Dearnaley[71], R. Debbe[25], C. Debenedetti[138], B. Dechenaux[55], D.V. Dedovich[64], I. Deigaard[106],
J. Del Peso[81], T. Del Prete[123a,123b], F. Deliot[137], C.M. Delitzsch[49], M. Deliyergiyev[74], A. Dell'Acqua[30],
L. Dell'Asta[22], M. Dell'Orso[123a,123b], M. Della Pietra[103a,j], d. della Volpe[49], M. Delmastro[5],
P.A. Delsart[55], C. Deluca[106], S. Demers[177], M. Demichev[64], A. Demilly[79], S.P. Denisov[129],

D. Derendarz[39], J.E. Derkaoui[136d], F. Derue[79], P. Dervan[73], K. Desch[21], C. Deterre[42], P.O. Deviveiros[106],
A. Dewhurst[130], S. Dhaliwal[106], A. Di Ciaccio[134a,134b], L. Di Ciaccio[5], A. Di Domenico[133a,133b],
C. Di Donato[103a,103b], A. Di Girolamo[30], B. Di Girolamo[30], A. Di Mattia[153], B. Di Micco[135a,135b],
R. Di Nardo[47], A. Di Simone[48], R. Di Sipio[20a,20b], D. Di Valentino[29], F.A. Dias[46], M.A. Diaz[32a],
E.B. Diehl[88], J. Dietrich[42], T.A. Dietzsch[58a], S. Diglio[84], A. Dimitrievska[13a], J. Dingfelder[21],
C. Dionisi[133a,133b], P. Dita[26a], S. Dita[26a], F. Dittus[30], F. Djama[84], T. Djobava[51b], J.I. Djuvsland[58a],
M.A.B. do Vale[24c], A. Do Valle Wemans[125a,125g], T.K.O. Doan[5], D. Dobos[30], C. Doglioni[49], T. Doherty[53],
T. Dohmae[156], J. Dolejsi[128], Z. Dolezal[128], B.A. Dolgoshein[97,*], M. Donadelli[24d], S. Donati[123a,123b],
P. Dondero[120a,120b], J. Donini[34], J. Dopke[130], A. Doria[103a], M.T. Dova[70], A.T. Doyle[53], M. Dris[10],
J. Dubbert[88], S. Dube[15], E. Dubreuil[34], E. Duchovni[173], G. Duckeck[99], O.A. Ducu[26a], D. Duda[176],
A. Dudarev[30], F. Dudziak[63], L. Duflot[116], L. Duguid[76], M. Dührssen[30], M. Dunford[58a], H. Duran Yildiz[4a],
M. Düren[52], A. Durglishvili[51b], M. Dwuznik[38a], M. Dyndal[38a], J. Ebke[99], W. Edson[2], N.C. Edwards[46],
W. Ehrenfeld[21], T. Eifert[144], G. Eigen[14], K. Einsweiler[15], T. Ekelof[167], M. El Kacimi[136c], M. Ellert[167],
S. Elles[5], F. Ellinghaus[82], N. Ellis[30], J. Elmsheuser[99], M. Elsing[30], D. Emeliyanov[130], Y. Enari[156],
O.C. Endner[82], M. Endo[117], R. Engelmann[149], J. Erdmann[177], A. Ereditato[17], D. Eriksson[147a],
G. Ernis[176], J. Ernst[2], M. Ernst[25], J. Ernwein[137], D. Errede[166], S. Errede[166], E. Ertel[82], M. Escalier[116],
H. Esch[43], C. Escobar[124], B. Esposito[47], A.I. Etienvre[137], E. Etzion[154], H. Evans[60], A. Ezhilov[122],
L. Fabbri[20a,20b], G. Facini[31], R.M. Fakhrutdinov[129], S. Falciano[133a], R.J. Falla[77], J. Faltova[128],
Y. Fang[33a], M. Fanti[90a,90b], A. Farbin[8], A. Farilla[135a], T. Farooque[12], S. Farrell[15], S.M. Farrington[171],
P. Farthouat[30], F. Fassi[136e], P. Fassnacht[30], D. Fassouliotis[9], A. Favareto[50a,50b], L. Fayard[116],
P. Federic[145a], O.L. Fedin[122,l], W. Fedorko[169], M. Fehling-Kaschek[48], S. Feigl[30], L. Feligioni[84], C. Feng[33d],
E.J. Feng[6], H. Feng[88], A.B. Fenyuk[129], S. Fernandez Perez[30], S. Ferrag[53], J. Ferrando[53], A. Ferrari[167],
P. Ferrari[106], R. Ferrari[120a], D.E. Ferreira de Lima[53], A. Ferrer[168], D. Ferrere[49], C. Ferretti[88],
A. Ferretto Parodi[50a,50b], M. Fiascaris[31], F. Fiedler[82], A. Filipčič[74], M. Filipuzzi[42], F. Filthaut[105],
M. Fincke-Keeler[170], K.D. Finelli[151], M.C.N. Fiolhais[125a,125c], L. Fiorini[168], A. Firan[40], A. Fischer[2],
J. Fischer[176], W.C. Fisher[89], E.A. Fitzgerald[23], M. Flechl[48], I. Fleck[142], P. Fleischmann[88],
S. Fleischmann[176], G.T. Fletcher[140], G. Fletcher[75], T. Flick[176], A. Floderus[80], L.R. Flores Castillo[174,m],
A.C. Florez Bustos[160b], M.J. Flowerdew[100], A. Formica[137], A. Forti[83], D. Fortin[160a], D. Fournier[116],
H. Fox[71], S. Fracchia[12], P. Francavilla[79], M. Franchini[20a,20b], S. Franchino[30], D. Francis[30], L. Franconi[118],
M. Franklin[57], S. Franz[61], M. Fraternali[120a,120b], S.T. French[28], C. Friedrich[42], F. Friedrich[44],
D. Froidevaux[30], J.A. Frost[28], C. Fukunaga[157], E. Fullana Torregrosa[82], B.G. Fulsom[144], J. Fuster[168],
C. Gabaldon[55], O. Gabizon[173], A. Gabrielli[20a,20b], A. Gabrielli[133a,133b], S. Gadatsch[106], S. Gadomski[49],
G. Gagliardi[50a,50b], P. Gagnon[60], C. Galea[105], B. Galhardo[125a,125c], E.J. Gallas[119], V. Gallo[17],
B.J. Gallop[130], P. Gallus[127], G. Galster[36], K.K. Gan[110], R.P. Gandrajula[62], J. Gao[33b], Y.S. Gao[144,f],
F.M. Garay Walls[46], F. Garberson[177], C. García[168], J.E. García Navarro[168], M. Garcia-Sciveres[15],
R.W. Gardner[31], N. Garelli[144], V. Garonne[30], C. Gatti[47], G. Gaudio[120a], B. Gaur[142], L. Gauthier[94],
P. Gauzzi[133a,133b], I.L. Gavrilenko[95], C. Gay[169], G. Gaycken[21], E.N. Gazis[10], P. Ge[33d], Z. Gecse[169],
C.N.P. Gee[130], D.A.A. Geerts[106], Ch. Geich-Gimbel[21], K. Gellerstedt[147a,147b], C. Gemme[50a],
A. Gemmell[53], M.H. Genest[55], S. Gentile[133a,133b], M. George[54], S. George[76], D. Gerbaudo[164],
A. Gershon[154], H. Ghazlane[136b], N. Ghodbane[34], B. Giacobbe[20a], S. Giagu[133a,133b], V. Giangiobbe[12],
P. Giannetti[123a,123b], F. Gianotti[30], B. Gibbard[25], S.M. Gibson[76], M. Gilchriese[15], T.P.S. Gillam[28],
D. Gillberg[30], G. Gilles[34], D.M. Gingrich[3,e], N. Giokaris[9], M.P. Giordani[165a,165c], R. Giordano[103a,103b],
F.M. Giorgi[20a], F.M. Giorgi[16], P.F. Giraud[137], D. Giugni[90a], C. Giuliani[48], M. Giulini[58b],
B.K. Gjelsten[118], S. Gkaitatzis[155], I. Gkialas[155], L.K. Gladilin[98], C. Glasman[81], J. Glatzer[30],
P.C.F. Glaysher[46], A. Glazov[42], G.L. Glonti[64], M. Goblirsch-Kolb[100], J.R. Goddard[75], J. Godfrey[143],
J. Godlewski[30], C. Goeringer[82], S. Goldfarb[88], T. Golling[177], D. Golubkov[129], A. Gomes[125a,125b,125d],
L.S. Gomez Fajardo[42], R. Gonçalo[125a], J. Goncalves Pinto Firmino Da Costa[137], L. Gonella[21],
S. González de la Hoz[168], G. Gonzalez Parra[12], S. Gonzalez-Sevilla[49], L. Goossens[30], P.A. Gorbounov[96],
H.A. Gordon[25], I. Gorelov[104], B. Gorini[30], E. Gorini[72a,72b], A. Gorišek[74], E. Gornicki[39], A.T. Goshaw[6],
C. Gössling[43], M.I. Gostkin[64], M. Gouighri[136a], D. Goujdami[136c], M.P. Goulette[49], A.G. Goussiou[139],
C. Goy[5], S. Gozpinar[23], H.M.X. Grabas[137], L. Graber[54], I. Grabowska-Bold[38a], P. Grafström[20a,20b],
K-J. Grahn[42], J. Gramling[49], E. Gramstad[118], S. Grancagnolo[16], V. Grassi[149], V. Gratchev[122],

17

H.M. Gray[30], E. Graziani[135a], O.G. Grebenyuk[122], Z.D. Greenwood[78,n], K. Gregersen[77], I.M. Gregor[42],
P. Grenier[144], J. Griffiths[8], A.A. Grillo[138], K. Grimm[71], S. Grinstein[12,o], Ph. Gris[34], Y.V. Grishkevich[98],
J.-F. Grivaz[116], J.P. Grohs[44], A. Grohsjean[42], E. Gross[173], J. Grosse-Knetter[54], G.C. Grossi[134a,134b],
J. Groth-Jensen[173], Z.J. Grout[150], L. Guan[33b], J. Guenther[127], F. Guescini[49], D. Guest[177], O. Gueta[154],
C. Guicheney[34], E. Guido[50a,50b], T. Guillemin[116], S. Guindon[2], U. Gul[53], C. Gumpert[44], J. Guo[35],
S. Gupta[119], P. Gutierrez[112], N.G. Gutierrez Ortiz[53], C. Gutschow[77], N. Guttman[154], C. Guyot[137],
C. Gwenlan[119], C.B. Gwilliam[73], A. Haas[109], C. Haber[15], H.K. Hadavand[8], N. Haddad[136e], P. Haefner[21],
S. Hageböck[21], Z. Hajduk[39], H. Hakobyan[178], M. Haleem[42], D. Hall[119], G. Halladjian[89], K. Hamacher[176],
P. Hamal[114], K. Hamano[170], M. Hamer[54], A. Hamilton[146a], S. Hamilton[162], G.N. Hamity[146c],
P.G. Hamnett[42], L. Han[33b], K. Hanagaki[117], K. Hanawa[156], M. Hance[15], P. Hanke[58a], R. Hanna[137],
J.B. Hansen[36], J.D. Hansen[36], P.H. Hansen[36], K. Hara[161], A.S. Hard[174], T. Harenberg[176], F. Hariri[116],
S. Harkusha[91], D. Harper[88], R.D. Harrington[46], O.M. Harris[139], P.F. Harrison[171], F. Hartjes[106],
M. Hasegawa[66], S. Hasegawa[102], Y. Hasegawa[141], A. Hasib[112], S. Hassani[137], S. Haug[17], M. Hauschild[30],
R. Hauser[89], M. Havranek[126], C.M. Hawkes[18], R.J. Hawkings[30], A.D. Hawkins[80], T. Hayashi[161],
D. Hayden[89], C.P. Hays[119], H.S. Hayward[73], S.J. Haywood[130], S.J. Head[18], T. Heck[82], V. Hedberg[80],
L. Heelan[8], S. Heim[121], T. Heim[176], B. Heinemann[15], L. Heinrich[109], J. Hejbal[126], L. Helary[22], C. Heller[99],
M. Heller[30], S. Hellman[147a,147b], D. Hellmich[21], C. Helsens[30], J. Henderson[119], R.C.W. Henderson[71],
Y. Heng[174], C. Hengler[42], A. Henrichs[177], A.M. Henriques Correia[30], S. Henrot-Versille[116], C. Hensel[54],
G.H. Herbert[16], Y. Hernández Jiménez[168], R. Herrberg-Schubert[16], G. Herten[48], R. Hertenberger[99],
L. Hervas[30], G.G. Hesketh[77], N.P. Hessey[106], R. Hickling[75], E. Higón-Rodriguez[168], E. Hill[170], J.C. Hill[28],
K.H. Hiller[42], S. Hillert[21], S.J. Hillier[18], I. Hinchliffe[15], E. Hines[121], M. Hirose[158], D. Hirschbuehl[176],
J. Hobbs[149], N. Hod[106], M.C. Hodgkinson[140], P. Hodgson[140], A. Hoecker[30], M.R. Hoeferkamp[104],
F. Hoenig[99], J. Hoffman[40], D. Hoffmann[84], M. Hohlfeld[82], T.R. Holmes[15], T.M. Hong[121],
L. Hooft van Huysduynen[109], J-Y. Hostachy[55], S. Hou[152], A. Hoummada[136a], J. Howard[119], J. Howarth[42],
M. Hrabovsky[114], I. Hristova[16], J. Hrivnac[116], T. Hryn'ova[5], C. Hsu[146c], P.J. Hsu[82], S.-C. Hsu[139], D. Hu[35],
X. Hu[88], Y. Huang[42], Z. Hubacek[30], F. Hubaut[84], F. Huegging[21], T.B. Huffman[119], E.W. Hughes[35],
G. Hughes[71], M. Huhtinen[30], T.A. Hülsing[82], M. Hurwitz[15], N. Huseynov[64,b], J. Huston[89], J. Huth[57],
G. Iacobucci[49], G. Iakovidis[10], I. Ibragimov[142], L. Iconomidou-Fayard[116], E. Ideal[177], P. Iengo[103a],
O. Igonkina[106], T. Iizawa[172], Y. Ikegami[65], K. Ikematsu[142], M. Ikeno[65], Y. Ilchenko[31,p], D. Iliadis[155],
N. Ilic[159], Y. Inamaru[66], T. Ince[100], P. Ioannou[9], M. Iodice[135a], K. Iordanidou[9], V. Ippolito[57],
A. Irles Quiles[168], C. Isaksson[167], M. Ishino[67], M. Ishitsuka[158], R. Ishmukhametov[110], C. Issever[119],
S. Istin[19a], J.M. Iturbe Ponce[83], R. Iuppa[134a,134b], J. Ivarsson[80], W. Iwanski[39], H. Iwasaki[65], J.M. Izen[41],
V. Izzo[103a], B. Jackson[121], M. Jackson[73], P. Jackson[1], M.R. Jaekel[30], V. Jain[2], K. Jakobs[48], S. Jakobsen[30],
T. Jakoubek[126], J. Jakubek[127], D.O. Jamin[152], D.K. Jana[78], E. Jansen[77], H. Jansen[30], J. Janssen[21],
M. Janus[171], G. Jarlskog[80], N. Javadov[64,b], T. Javůrek[48], L. Jeanty[15], J. Jejelava[51a,q], G.-Y. Jeng[151],
D. Jennens[87], P. Jenni[48,r], J. Jentzsch[43], C. Jeske[171], S. Jézéquel[5], H. Ji[174], J. Jia[149], Y. Jiang[33b],
M. Jimenez Belenguer[42], S. Jin[33a], A. Jinaru[26a], O. Jinnouchi[158], M.D. Joergensen[36],
K.E. Johansson[147a,147b], P. Johansson[140], K.A. Johns[7], K. Jon-And[147a,147b], G. Jones[171], R.W.L. Jones[71],
T.J. Jones[73], J. Jongmanns[58a], P.M. Jorge[125a,125b], K.D. Joshi[83], J. Jovicevic[148], X. Ju[174], C.A. Jung[43],
R.M. Jungst[30], P. Jussel[61], A. Juste Rozas[12,o], M. Kaci[168], A. Kaczmarska[39], M. Kado[116], H. Kagan[110],
M. Kagan[144], E. Kajomovitz[45], C.W. Kalderon[119], S. Kama[40], A. Kamenshchikov[129], N. Kanaya[156],
M. Kaneda[30], S. Kaneti[28], V.A. Kantserov[97], J. Kanzaki[65], B. Kaplan[109], A. Kapliy[31], D. Kar[53],
K. Karakostas[10], N. Karastathis[10], M. Karnevskiy[82], S.N. Karpov[64], Z.M. Karpova[64], K. Karthik[109],
V. Kartvelishvili[71], A.N. Karyukhin[129], L. Kashif[174], G. Kasieczka[58b], R.D. Kass[110], A. Kastanas[14],
Y. Kataoka[156], A. Katre[49], J. Katzy[42], V. Kaushik[7], K. Kawagoe[69], T. Kawamoto[156], G. Kawamura[54],
S. Kazama[156], V.F. Kazanin[108], M.Y. Kazarinov[64], R. Keeler[170], R. Kehoe[40], M. Keil[54], J.S. Keller[42],
J.J. Kempster[76], H. Keoshkerian[5], O. Kepka[126], B.P. Kerševan[74], S. Kersten[176], K. Kessoku[156],
J. Keung[159], F. Khalil-zada[11], H. Khandanyan[147a,147b], A. Khanov[113], A. Khodinov[97], A. Khomich[58a],
T.J. Khoo[28], G. Khoriauli[21], A. Khoroshilov[176], V. Khovanskiy[96], E. Khramov[64], J. Khubua[51b],
H.Y. Kim[8], H. Kim[147a,147b], S.H. Kim[161], N. Kimura[172], O. Kind[16], B.T. King[73], M. King[168],
R.S.B. King[119], S.B. King[169], J. Kirk[130], A.E. Kiryunin[100], T. Kishimoto[66], D. Kisielewska[38a], F. Kiss[48],
T. Kittelmann[124], K. Kiuchi[161], E. Kladiva[145b], M. Klein[73], U. Klein[73], K. Kleinknecht[82],

P. Klimek[147a,147b], A. Klimentov[25], R. Klingenberg[43], J.A. Klinger[83], T. Klioutchnikova[30], P.F. Klok[105], E.-E. Kluge[58a], P. Kluit[106], S. Kluth[100], E. Kneringer[61], E.B.F.G. Knoops[84], A. Knue[53], D. Kobayashi[158], T. Kobayashi[156], M. Kobel[44], M. Kocian[144], P. Kodys[128], P. Koevesarki[21], T. Koffas[29], E. Koffeman[106], L.A. Kogan[119], S. Kohlmann[176], Z. Kohout[127], T. Kohriki[65], T. Koi[144], H. Kolanoski[16], I. Koletsou[5], J. Koll[89], A.A. Komar[95,*], Y. Komori[156], T. Kondo[65], N. Kondrashova[42], K. Köneke[48], A.C. König[105], S. König[82], T. Kono[65,s], R. Konoplich[109,t], N. Konstantinidis[77], R. Kopeliansky[153], S. Koperny[38a], L. Köpke[82], A.K. Kopp[48], K. Korcyl[39], K. Kordas[155], A. Korn[77], A.A. Korol[108,c], I. Korolkov[12], E.V. Korolkova[140], V.A. Korotkov[129], O. Kortner[100], S. Kortner[100], V.V. Kostyukhin[21], V.M. Kotov[64], A. Kotwal[45], C. Kourkoumelis[9], V. Kouskoura[155], A. Koutsman[160a], R. Kowalewski[170], T.Z. Kowalski[38a], W. Kozanecki[137], A.S. Kozhin[129], V. Kral[127], V.A. Kramarenko[98], G. Kramberger[74], D. Krasnopevtsev[97], M.W. Krasny[79], A. Krasznahorkay[30], J.K. Kraus[21], A. Kravchenko[25], S. Kreiss[109], M. Kretz[58c], J. Kretzschmar[73], K. Kreutzfeldt[52], P. Krieger[159], K. Kroeninger[54], H. Kroha[100], J. Kroll[121], J. Kroseberg[21], J. Krstic[13a], U. Kruchonak[64], H. Krüger[21], T. Kruker[17], N. Krumnack[63], Z.V. Krumshteyn[64], A. Kruse[174], M.C. Kruse[45], M. Kruskal[22], T. Kubota[87], S. Kuday[4a], S. Kuehn[48], A. Kugel[58c], A. Kuhl[138], T. Kuhl[42], V. Kukhtin[64], Y. Kulchitsky[91], S. Kuleshov[32b], M. Kuna[133a,133b], J. Kunkle[121], A. Kupco[126], H. Kurashige[66], Y.A. Kurochkin[91], R. Kurumida[66], V. Kus[126], E.S. Kuwertz[148], M. Kuze[158], J. Kvita[114], A. La Rosa[49], L. La Rotonda[37a,37b], C. Lacasta[168], F. Lacava[133a,133b], J. Lacey[29], H. Lacker[16], D. Lacour[79], V.R. Lacuesta[168], E. Ladygin[64], R. Lafaye[5], B. Laforge[79], T. Lagouri[177], S. Lai[48], H. Laier[58a], L. Lambourne[77], S. Lammers[60], C.L. Lampen[7], W. Lampl[7], E. Lançon[137], U. Landgraf[48], M.P.J. Landon[75], V.S. Lang[58a], A.J. Lankford[164], F. Lanni[25], K. Lantzsch[30], S. Laplace[79], C. Lapoire[21], J.F. Laporte[137], T. Lari[90a], M. Lassnig[30], P. Laurelli[47], W. Lavrijsen[15], A.T. Law[138], P. Laycock[73], O. Le Dortz[79], E. Le Guirriec[84], E. Le Menedeu[12], T. LeCompte[6], F. Ledroit-Guillon[55], C.A. Lee[152], H. Lee[106], J.S.H. Lee[117], S.C. Lee[152], L. Lee[177], G. Lefebvre[79], M. Lefebvre[170], F. Legger[99], C. Leggett[15], A. Lehan[73], M. Lehmacher[21], G. Lehmann Miotto[30], X. Lei[7], W.A. Leight[29], A. Leisos[155], A.G. Leister[177], M.A.L. Leite[24d], R. Leitner[128], D. Lellouch[173], B. Lemmer[54], K.J.C. Leney[77], T. Lenz[21], G. Lenzen[176], B. Lenzi[30], R. Leone[7], S. Leone[123a,123b], K. Leonhardt[44], C. Leonidopoulos[46], S. Leontsinis[10], C. Leroy[94], C.G. Lester[28], C.M. Lester[121], M. Levchenko[122], J. Levêque[5], D. Levin[88], L.J. Levinson[173], M. Levy[18], A. Lewis[119], G.H. Lewis[109], A.M. Leyko[21], M. Leyton[41], B. Li[33b,u], B. Li[84], H. Li[149], H.L. Li[31], L. Li[45], L. Li[33e], S. Li[45], Y. Li[33c,v], Z. Liang[138], H. Liao[34], B. Liberti[134a], P. Lichard[30], K. Lie[166], J. Liebal[21], W. Liebig[14], C. Limbach[21], A. Limosani[87], S.C. Lin[152,w], T.H. Lin[82], F. Linde[106], B.E. Lindquist[149], J.T. Linnemann[89], E. Lipeles[121], A. Lipniacka[14], M. Lisovyi[42], T.M. Liss[166], D. Lissauer[25], A. Lister[169], A.M. Litke[138], B. Liu[152], D. Liu[152], J.B. Liu[33b], K. Liu[33b,x], L. Liu[88], M. Liu[45], M. Liu[33b], Y. Liu[33b], M. Livan[120a,120b], S.S.A. Livermore[119], A. Lleres[55], J. Llorente Merino[81], S.L. Lloyd[75], F. Lo Sterzo[152], E. Lobodzinska[42], P. Loch[7], W.S. Lockman[138], F.K. Loebinger[83], A.E. Loevschall-Jensen[36], A. Loginov[177], T. Lohse[16], K. Lohwasser[42], M. Lokajicek[126], V.P. Lombardo[5], B.A. Long[22], J.D. Long[88], R.E. Long[71], L. Lopes[125a], D. Lopez Mateos[57], B. Lopez Paredes[140], I. Lopez Paz[12], J. Lorenz[99], N. Lorenzo Martinez[60], M. Losada[163], P. Loscutoff[15], X. Lou[41], A. Lounis[116], J. Love[6], P.A. Love[71], A.J. Lowe[144,f], F. Lu[33a], N. Lu[88], H.J. Lubatti[139], C. Luci[133a,133b], A. Lucotte[55], F. Luehring[60], W. Lukas[61], L. Luminari[133a], O. Lundberg[147a,147b], B. Lund-Jensen[148], M. Lungwitz[82], D. Lynn[25], R. Lysak[126], E. Lytken[80], H. Ma[25], L.L. Ma[33d], G. Maccarrone[47], A. Macchiolo[100], J. Machado Miguens[125a,125b], D. Macina[30], D. Madaffari[84], R. Madar[48], H.J. Maddocks[71], W.F. Mader[44], A. Madsen[167], M. Maeno[8], T. Maeno[25], E. Magradze[54], K. Mahboubi[48], J. Mahlstedt[106], S. Mahmoud[73], C. Maiani[137], C. Maidantchik[24a], A.A. Maier[100], A. Maio[125a,125b,125d], S. Majewski[115], Y. Makida[65], N. Makovec[116], P. Mal[137,y], B. Malaescu[79], Pa. Malecki[39], V.P. Maleev[122], F. Malek[55], U. Mallik[62], D. Malon[6], C. Malone[144], S. Maltezos[10], V.M. Malyshev[108], S. Malyukov[30], J. Mamuzic[13b], B. Mandelli[30], L. Mandelli[90a], I. Mandić[74], R. Mandrysch[62], J. Maneira[125a,125b], A. Manfredini[100], L. Manhaes de Andrade Filho[24b], J. Manjarres Ramos[160b], A. Mann[99], P.M. Manning[138], A. Manousakis-Katsikakis[9], B. Mansoulie[137], R. Mantifel[86], L. Mapelli[30], L. March[146c], J.F. Marchand[29], G. Marchiori[79], M. Marcisovsky[126], C.P. Marino[170], M. Marjanovic[13a], C.N. Marques[125a], F. Marroquim[24a], S.P. Marsden[83], Z. Marshall[15], L.F. Marti[17], S. Marti-Garcia[168], B. Martin[30], B. Martin[89], T.A. Martin[171], V.J. Martin[46], B. Martin dit Latour[14], H. Martinez[137], M. Martinez[12,o], S. Martin-Haugh[130], A.C. Martyniuk[77],

M. Marx[139], F. Marzano[133a], A. Marzin[30], L. Masetti[82], T. Mashimo[156], R. Mashinistov[95], J. Masik[83],
A.L. Maslennikov[108,c], I. Massa[20a,20b], L. Massa[20a,20b], N. Massol[5], P. Mastrandrea[149],
A. Mastroberardino[37a,37b], T. Masubuchi[156], P. Mättig[176], J. Mattmann[82], J. Maurer[26a], S.J. Maxfield[73],
D.A. Maximov[108,c], R. Mazini[152], L. Mazzaferro[134a,134b], G. Mc Goldrick[159], S.P. Mc Kee[88], A. McCarn[88],
R.L. McCarthy[149], T.G. McCarthy[29], N.A. McCubbin[130], K.W. McFarlane[56,*], J.A. Mcfayden[77],
G. Mchedlidze[54], S.J. McMahon[130], R.A. McPherson[170,k], A. Meade[85], J. Mechnich[106], M. Medinnis[42],
S. Meehan[31], S. Mehlhase[99], A. Mehta[73], K. Meier[58a], C. Meineck[99], B. Meirose[80], C. Melachrinos[31],
B.R. Mellado Garcia[146c], F. Meloni[17], A. Mengarelli[20a,20b], S. Menke[100], E. Meoni[162], K.M. Mercurio[57],
S. Mergelmeyer[21], N. Meric[137], P. Mermod[49], L. Merola[103a,103b], C. Meroni[90a], F.S. Merritt[31],
H. Merritt[110], A. Messina[30,z], J. Metcalfe[25], A.S. Mete[164], C. Meyer[82], C. Meyer[121], J-P. Meyer[137],
J. Meyer[30], R.P. Middleton[130], S. Migas[73], L. Mijović[21], G. Mikenberg[173], M. Mikestikova[126], M. Mikuž[74],
A. Milic[30], D.W. Miller[31], C. Mills[46], A. Milov[173], D.A. Milstead[147a,147b], D. Milstein[173],
A.A. Minaenko[129], I.A. Minashvili[64], A.I. Mincer[109], B. Mindur[38a], M. Mineev[64], Y. Ming[174], L.M. Mir[12],
G. Mirabelli[133a], T. Mitani[172], J. Mitrevski[99], V.A. Mitsou[168], S. Mitsui[65], A. Miucci[49], P.S. Miyagawa[140],
J.U. Mjörnmark[80], T. Moa[147a,147b], K. Mochizuki[84], S. Mohapatra[35], W. Mohr[48], S. Molander[147a,147b],
R. Moles-Valls[168], K. Mönig[42], C. Monini[55], J. Monk[36], E. Monnier[84], J. Montejo Berlingen[12],
F. Monticelli[70], S. Monzani[133a,133b], R.W. Moore[3], A. Moraes[53], N. Morange[62], D. Moreno[82],
M. Moreno Llácer[54], P. Morettini[50a], M. Morgenstern[44], M. Morii[57], S. Moritz[82], A.K. Morley[148],
G. Mornacchi[30], J.D. Morris[75], L. Morvaj[102], H.G. Moser[100], M. Mosidze[51b], J. Moss[110], K. Motohashi[158],
R. Mount[144], E. Mountricha[25], S.V. Mouraviev[95,*], E.J.W. Moyse[85], S. Muanza[84], R.D. Mudd[18],
F. Mueller[58a], J. Mueller[124], K. Mueller[21], T. Mueller[28], T. Mueller[82], D. Muenstermann[49], Y. Munwes[154],
J.A. Murillo Quijada[18], W.J. Murray[171,130], H. Musheghyan[54], E. Musto[153], A.G. Myagkov[129,aa],
M. Myska[127], O. Nackenhorst[54], J. Nadal[54], K. Nagai[61], R. Nagai[158], Y. Nagai[84], K. Nagano[65],
A. Nagarkar[110], Y. Nagasaka[59], M. Nagel[100], A.M. Nairz[30], Y. Nakahama[30], K. Nakamura[65],
T. Nakamura[156], I. Nakano[111], H. Namasivayam[41], G. Nanava[21], R. Narayan[58b], T. Nattermann[21],
T. Naumann[42], G. Navarro[163], R. Nayyar[7], H.A. Neal[88], P.Yu. Nechaeva[95], T.J. Neep[83], P.D. Nef[144],
A. Negri[120a,120b], G. Negri[30], M. Negrini[20a], S. Nektarijevic[49], A. Nelson[164], T.K. Nelson[144],
S. Nemecek[126], P. Nemethy[109], A.A. Nepomuceno[24a], M. Nessi[30,ab], M.S. Neubauer[166], M. Neumann[176],
R.M. Neves[109], P. Nevski[25], P.R. Newman[18], D.H. Nguyen[6], R.B. Nickerson[119], R. Nicolaidou[137],
B. Nicquevert[30], J. Nielsen[138], N. Nikiforou[35], A. Nikiforov[16], V. Nikolaenko[129,aa], I. Nikolic-Audit[79],
K. Nikolics[49], K. Nikolopoulos[18], P. Nilsson[8], Y. Ninomiya[156], A. Nisati[133a], R. Nisius[100], T. Nobe[158],
L. Nodulman[6], M. Nomachi[117], I. Nomidis[29], S. Norberg[112], M. Nordberg[30], O. Novgorodova[44],
S. Nowak[100], M. Nozaki[65], L. Nozka[114], K. Ntekas[10], G. Nunes Hanninger[87], T. Nunnemann[99], E. Nurse[77],
F. Nuti[87], B.J. O'Brien[46], F. O'grady[7], D.C. O'Neil[143], V. O'Shea[53], F.G. Oakham[29,e], H. Oberlack[100],
T. Obermann[21], J. Ocariz[79], A. Ochi[66], I. Ochoa[77], S. Oda[69], S. Odaka[65], H. Ogren[60], A. Oh[83], S.H. Oh[45],
C.C. Ohm[15], H. Ohman[167], W. Okamura[117], H. Okawa[25], Y. Okumura[31], T. Okuyama[156], A. Olariu[26a],
A.G. Olchevski[64], S.A. Olivares Pino[46], D. Oliveira Damazio[25], E. Oliver Garcia[168], A. Olszewski[39],
J. Olszowska[39], A. Onofre[125a,125e], P.U.E. Onyisi[31,p], C.J. Oram[160a], M.J. Oreglia[31], Y. Oren[154],
D. Orestano[135a,135b], N. Orlando[72a,72b], C. Oropeza Barrera[53], R.S. Orr[159], B. Osculati[50a,50b],
R. Ospanov[121], G. Otero y Garzon[27], H. Otono[69], M. Ouchrif[136d], E.A. Ouellette[170], F. Ould-Saada[118],
A. Ouraou[137], K.P. Oussoren[106], Q. Ouyang[33a], A. Ovcharova[15], M. Owen[83], V.E. Ozcan[19a], N. Ozturk[8],
K. Pachal[119], A. Pacheco Pages[12], C. Padilla Aranda[12], M. Pagáčová[48], S. Pagan Griso[15], E. Paganis[140],
C. Pahl[100], F. Paige[25], P. Pais[85], K. Pajchel[118], G. Palacino[160b], S. Palestini[30], M. Palka[38b], D. Pallin[34],
A. Palma[125a,125b], J.D. Palmer[18], Y.B. Pan[174], E. Panagiotopoulou[10], J.G. Panduro Vazquez[76], P. Pani[106],
N. Panikashvili[88], S. Panitkin[25], D. Pantea[26a], L. Paolozzi[134a,134b], Th.D. Papadopoulou[10],
K. Papageorgiou[155], A. Paramonov[6], D. Paredes Hernandez[34], M.A. Parker[28], F. Parodi[50a,50b],
J.A. Parsons[35], U. Parzefall[48], E. Pasqualucci[133a], S. Passaggio[50a], A. Passeri[135a], F. Pastore[135a,135b,*],
Fr. Pastore[76], G. Pásztor[29], S. Pataraia[176], N.D. Patel[151], J.R. Pater[83], S. Patricelli[103a,103b], T. Pauly[30],
J. Pearce[170], M. Pedersen[118], S. Pedraza Lopez[168], R. Pedro[125a,125b], S.V. Peleganchuk[108], D. Pelikan[167],
H. Peng[33b], B. Penning[31], J. Penwell[60], D.V. Perepelitsa[25], E. Perez Codina[160a],
M.T. Pérez García-Estañ[168], V. Perez Reale[35], L. Perini[90a,90b], H. Pernegger[30], R. Perrino[72a],
R. Peschke[42], V.D. Peshekhonov[64], K. Peters[30], R.F.Y. Peters[83], B.A. Petersen[30], T.C. Petersen[36],

E. Petit[42], A. Petridis[147a,147b], C. Petridou[155], E. Petrolo[133a], F. Petrucci[135a,135b], N.E. Pettersson[158],
R. Pezoa[32b], P.W. Phillips[130], G. Piacquadio[144], E. Pianori[171], A. Picazio[49], E. Piccaro[75],
M. Piccinini[20a,20b], R. Piegaia[27], D.T. Pignotti[110], J.E. Pilcher[31], A.D. Pilkington[77], J. Pina[125a,125b,125d],
M. Pinamonti[165a,165c,ac], A. Pinder[119], J.L. Pinfold[3], A. Pingel[36], B. Pinto[125a], S. Pires[79], M. Pitt[173],
C. Pizio[90a,90b], L. Plazak[145a], M.-A. Pleier[25], V. Pleskot[128], E. Plotnikova[64], P. Plucinski[147a,147b],
S. Poddar[58a], F. Podlyski[34], R. Poettgen[82], L. Poggioli[116], D. Pohl[21], M. Pohl[49], G. Polesello[120a],
A. Policicchio[37a,37b], R. Polifka[159], A. Polini[20a], C.S. Pollard[45], V. Polychronakos[25], K. Pommès[30],
L. Pontecorvo[133a], B.G. Pope[89], G.A. Popeneciu[26b], D.S. Popovic[13a], A. Poppleton[30], X. Portell Bueso[12],
S. Pospisil[127], K. Potamianos[15], I.N. Potrap[64], C.J. Potter[150], C.T. Potter[115], G. Poulard[30], J. Poveda[60],
V. Pozdnyakov[64], P. Pralavorio[84], A. Pranko[15], S. Prasad[30], R. Pravahan[8], S. Prell[63], D. Price[83],
J. Price[73], L.E. Price[6], L.E. Prieur[124], M. Primavera[72a], M. Proissl[46], K. Prokofiev[47], F. Prokoshin[32b],
E. Protopapadaki[137], S. Protopopescu[25], J. Proudfoot[6], M. Przybycien[38a], H. Przysieзниак[5], E. Ptacek[115],
D. Puddu[135a,135b], E. Pueschel[85], D. Puldon[149], M. Purohit[25,ad], P. Puzo[116], J. Qian[88], G. Qin[53],
Y. Qin[83], A. Quadt[54], D.R. Quarrie[15], W.B. Quayle[165a,165b], M. Queitsch-Maitland[83], D. Quilty[53],
A. Qureshi[160b], V. Radeka[25], V. Radescu[42], S.K. Radhakrishnan[149], P. Radloff[115], P. Rados[87],
F. Ragusa[90a,90b], G. Rahal[179], S. Rajagopalan[25], M. Rammensee[30], A.S. Randle-Conde[40],
C. Rangel-Smith[167], K. Rao[164], F. Rauscher[99], T.C. Rave[48], T. Ravenscroft[53], M. Raymond[30],
A.L. Read[118], N.P. Readioff[73], D.M. Rebuzzi[120a,120b], A. Redelbach[175], G. Redlinger[25], R. Reece[138],
K. Reeves[41], L. Rehnisch[16], H. Reisin[27], M. Relich[164], C. Rembser[30], H. Ren[33a], Z.L. Ren[152],
A. Renaud[116], M. Rescigno[133a], S. Resconi[90a], O.L. Rezanova[108,c], P. Reznicek[128], R. Rezvani[94],
R. Richter[100], M. Ridel[79], P. Rieck[16], J. Rieger[54], M. Rijssenbeek[149], A. Rimoldi[120a,120b], L. Rinaldi[20a],
E. Ritsch[61], I. Riu[12], F. Rizatdinova[113], E. Rizvi[75], S.H. Robertson[86,k], A. Robichaud-Veronneau[86],
D. Robinson[28], J.E.M. Robinson[83], A. Robson[53], C. Roda[123a,123b], L. Rodrigues[30], S. Roe[30], O. Røhne[118],
S. Rolli[162], A. Romaniouk[97], M. Romano[20a,20b], E. Romero Adam[168], N. Rompotis[139], M. Ronzani[48],
L. Roos[79], E. Ros[168], S. Rosati[133a], K. Rosbach[49], M. Rose[76], P. Rose[138], P.L. Rosendahl[14],
O. Rosenthal[142], V. Rossetti[147a,147b], E. Rossi[103a,103b], L.P. Rossi[50a], R. Rosten[139], M. Rotaru[26a],
I. Roth[173], J. Rothberg[139], D. Rousseau[116], C.R. Royon[137], A. Rozanov[84], Y. Rozen[153], X. Ruan[146c],
F. Rubbo[12], I. Rubinskiy[42], V.I. Rud[98], C. Rudolph[44], M.S. Rudolph[159], F. Rühr[48], A. Ruiz-Martinez[30],
Z. Rurikova[48], N.A. Rusakovich[64], A. Ruschke[99], J.P. Rutherfoord[7], N. Ruthmann[48], Y.F. Ryabov[122],
M. Rybar[128], G. Rybkin[116], N.C. Ryder[119], A.F. Saavedra[151], S. Sacerdoti[27], A. Saddique[3], I. Sadeh[154],
H.F-W. Sadrozinski[138], R. Sadykov[64], F. Safai Tehrani[133a], H. Sakamoto[156], Y. Sakurai[172],
G. Salamanna[135a,135b], A. Salamon[134a], M. Saleem[112], D. Salek[106], P.H. Sales De Bruin[139], D. Salihagic[100],
A. Salnikov[144], J. Salt[168], D. Salvatore[37a,37b], F. Salvatore[150], A. Salvucci[105], A. Salzburger[30],
D. Sampsonidis[155], A. Sanchez[103a,103b], J. Sánchez[168], V. Sanchez Martinez[168], H. Sandaker[14],
R.L. Sandbach[75], H.G. Sander[82], M.P. Sanders[99], M. Sandhoff[176], T. Sandoval[28], C. Sandoval[163],
R. Sandstroem[100], D.P.C. Sankey[130], A. Sansoni[47], C. Santoni[34], R. Santonico[134a,134b], H. Santos[125a],
I. Santoyo Castillo[150], K. Sapp[124], A. Sapronov[64], J.G. Saraiva[125a,125d], B. Sarrazin[21], G. Sartisohn[176],
O. Sasaki[65], Y. Sasaki[156], G. Sauvage[5,*], E. Sauvan[5], P. Savard[159,e], D.O. Savu[30], C. Sawyer[119],
L. Sawyer[78,n], D.H. Saxon[53], J. Saxon[121], C. Sbarra[20a], A. Sbrizzi[3], T. Scanlon[77], D.A. Scannicchio[164],
M. Scarcella[151], V. Scarfone[37a,37b], J. Schaarschmidt[173], P. Schacht[100], D. Schaefer[30], R. Schaefer[42],
S. Schaepe[21], S. Schaetzel[58b], U. Schäfer[82], A.C. Schaffer[116], D. Schaile[99], R.D. Schamberger[149],
V. Scharf[58a], V.A. Schegelsky[122], D. Scheirich[128], M. Schernau[164], M.I. Scherzer[35], C. Schiavi[50a,50b],
J. Schieck[99], C. Schillo[48], M. Schioppa[37a,37b], S. Schlenker[30], E. Schmidt[48], K. Schmieden[30], C. Schmitt[82],
S. Schmitt[58b], B. Schneider[17], Y.J. Schnellbach[73], U. Schnoor[44], L. Schoeffel[137], A. Schoening[58b],
B.D. Schoenrock[89], A.L.S. Schorlemmer[54], M. Schott[82], D. Schouten[160a], J. Schovancova[25],
S. Schramm[159], M. Schreyer[175], C. Schroeder[82], N. Schuh[82], M.J. Schultens[21], H.-C. Schultz-Coulon[58a],
H. Schulz[16], M. Schumacher[48], B.A. Schumm[138], Ph. Schune[137], C. Schwanenberger[83], A. Schwartzman[144],
Ph. Schwegler[100], Ph. Schwemling[137], R. Schwienhorst[89], J. Schwindling[137], T. Schwindt[21], M. Schwoerer[5],
F.G. Sciacca[17], E. Scifo[116], G. Sciolla[23], W.G. Scott[130], F. Scuri[123a,123b], F. Scutti[21], J. Searcy[88],
G. Sedov[42], E. Sedykh[122], S.C. Seidel[104], A. Seiden[138], F. Seifert[127], J.M. Seixas[24a], G. Sekhniaidze[103a],
S.J. Sekula[40], K.E. Selbach[46], D.M. Seliverstov[122,*], G. Sellers[73], N. Semprini-Cesari[20a,20b], C. Serfon[30],
L. Serin[116], L. Serkin[54], T. Serre[84], R. Seuster[160a], H. Severini[112], T. Sfiligoj[74], F. Sforza[100], A. Sfyrla[30],

21

E. Shabalina[54], M. Shamim[115], L.Y. Shan[33a], R. Shang[166], J.T. Shank[22], M. Shapiro[15], P.B. Shatalov[96], K. Shaw[165a,165b], C.Y. Shehu[150], P. Sherwood[77], L. Shi[152,ae], S. Shimizu[66], C.O. Shimmin[164], M. Shimojima[101], M. Shiyakova[64], A. Shmeleva[95], M.J. Shochet[31], D. Short[119], S. Shrestha[63], E. Shulga[97], M.A. Shupe[7], S. Shushkevich[42], P. Sicho[126], O. Sidiropoulou[155], D. Sidorov[113], A. Sidoti[133a], F. Siegert[44], Dj. Sijacki[13a], J. Silva[125a,125d], Y. Silver[154], D. Silverstein[144], S.B. Silverstein[147a], V. Simak[127], O. Simard[5], Lj. Simic[13a], S. Simion[116], E. Simioni[82], B. Simmons[77], R. Simoniello[90a,90b], M. Simonyan[36], P. Sinervo[159], N.B. Sinev[115], V. Sipica[142], G. Siragusa[175], A. Sircar[78], A.N. Sisakyan[64,∗], S.Yu. Sivoklokov[98], J. Sjölin[147a,147b], T.B. Sjursen[14], H.P. Skottowe[57], K.Yu. Skovpen[108], P. Skubic[112], M. Slater[18], T. Slavicek[127], K. Sliwa[162], V. Smakhtin[173], B.H. Smart[46], L. Smestad[14], S.Yu. Smirnov[97], Y. Smirnov[97], L.N. Smirnova[98,af], O. Smirnova[80], K.M. Smith[53], M. Smizanska[71], K. Smolek[127], A.A. Snesarev[95], G. Snidero[75], S. Snyder[25], R. Sobie[170,k], F. Socher[44], A. Soffer[154], D.A. Soh[152,ae], C.A. Solans[30], M. Solar[127], J. Solc[127], E.Yu. Soldatov[97], U. Soldevila[168], A.A. Solodkov[129], A. Soloshenko[64], O.V. Solovyanov[129], V. Solovyev[122], P. Sommer[48], H.Y. Song[33b], N. Soni[1], A. Sood[15], A. Sopczak[127], B. Sopko[127], V. Sopko[127], V. Sorin[12], M. Sosebee[8], R. Soualah[165a,165c], P. Soueid[94], A.M. Soukharev[108,c], D. South[42], S. Spagnolo[72a,72b], F. Spanò[76], W.R. Spearman[57], F. Spettel[100], R. Spighi[20a], G. Spigo[30], L.A. Spiller[87], M. Spousta[128], T. Spreitzer[159], B. Spurlock[8], R.D. St. Denis[53,∗], S. Staerz[44], J. Stahlman[121], R. Stamen[58a], S. Stamm[16], E. Stanecka[39], R.W. Stanek[6], C. Stanescu[135a], M. Stanescu-Bellu[42], M.M. Stanitzki[42], S. Stapnes[118], E.A. Starchenko[129], J. Stark[55], P. Staroba[126], P. Starovoitov[42], R. Staszewski[39], P. Stavina[145a,∗], P. Steinberg[25], B. Stelzer[143], H.J. Stelzer[30], O. Stelzer-Chilton[160a], H. Stenzel[52], S. Stern[100], G.A. Stewart[53], J.A. Stillings[21], M.C. Stockton[86], M. Stoebe[86], G. Stoicea[26a], P. Stolte[54], S. Stonjek[100], A.R. Stradling[8], A. Straessner[44], M.E. Stramaglia[17], J. Strandberg[148], S. Strandberg[147a,147b], A. Strandlie[118], E. Strauss[144], M. Strauss[112], P. Strizenec[145b], R. Ströhmer[175], D.M. Strom[115], R. Stroynowski[40], S.A. Stucci[17], B. Stugu[14], N.A. Styles[42], D. Su[144], J. Su[124], R. Subramaniam[78], A. Succurro[12], Y. Sugaya[117], C. Suhr[107], M. Suk[127], V.V. Sulin[95], S. Sultansoy[4c], T. Sumida[67], S. Sun[57], X. Sun[33a], J.E. Sundermann[48], K. Suruliz[140], G. Susinno[37a,37b], M.R. Sutton[150], Y. Suzuki[65], M. Svatos[126], S. Swedish[169], M. Swiatlowski[144], I. Sykora[145a], T. Sykora[128], D. Ta[89], C. Taccini[135a,135b], K. Tackmann[42], J. Taenzer[159], A. Taffard[164], R. Tafirout[160a], N. Taiblum[154], H. Takai[25], R. Takashima[68], H. Takeda[66], T. Takeshita[141], Y. Takubo[65], M. Talby[84], A.A. Talyshev[108,c], J.Y.C. Tam[175], K.G. Tan[87], J. Tanaka[156], R. Tanaka[116], S. Tanaka[132], S. Tanaka[65], A.J. Tanasijczuk[143], B.B. Tannenwald[110], N. Tannoury[21], S. Tapprogge[82], S. Tarem[153], F. Tarrade[29], G.F. Tartarelli[90a], P. Tas[128], M. Tasevsky[126], T. Tashiro[67], E. Tassi[37a,37b], A. Tavares Delgado[125a,125b], Y. Tayalati[136d], F.E. Taylor[93], G.N. Taylor[87], W. Taylor[160b], F.A. Teischinger[30], M. Teixeira Dias Castanheira[75], P. Teixeira-Dias[76], K.K. Temming[48], H. Ten Kate[30], P.K. Teng[152], J.J. Teoh[117], S. Terada[65], K. Terashi[156], J. Terron[81], S. Terzo[100], M. Testa[47], R.J. Teuscher[159,k], J. Therhaag[21], T. Theveneaux-Pelzer[34], J.P. Thomas[18], J. Thomas-Wilsker[76], E.N. Thompson[35], P.D. Thompson[18], P.D. Thompson[159], R.J. Thompson[83], A.S. Thompson[53], L.A. Thomsen[36], E. Thomson[121], M. Thomson[28], W.M. Thong[87], R.P. Thun[88,∗], F. Tian[35], M.J. Tibbetts[15], V.O. Tikhomirov[95,ag], Yu.A. Tikhonov[108,c], S. Timoshenko[97], E. Tiouchichine[84], P. Tipton[177], S. Tisserant[84], T. Todorov[5,∗], S. Todorova-Nova[128], B. Toggerson[7], J. Tojo[69], S. Tokár[145a], K. Tokushuku[65], K. Tollefson[89], L. Tomlinson[83], M. Tomoto[102], L. Tompkins[31], K. Toms[104], N.D. Topilin[64], E. Torrence[115], H. Torres[143], E. Torró Pastor[168], J. Toth[84,ah], F. Touchard[84], D.R. Tovey[140], H.L. Tran[116], T. Trefzger[175], L. Tremblet[30], A. Tricoli[30], I.M. Trigger[160a], S. Trincaz-Duvoid[79], M.F. Tripiana[12], W. Trischuk[159], B. Trocmé[55], C. Troncon[90a], M. Trottier-McDonald[143], M. Trovatelli[135a,135b], P. True[89], M. Trzebinski[39], A. Trzupek[39], C. Tsarouchas[30], J.C-L. Tseng[119], P.V. Tsiareshka[91], D. Tsionou[137], G. Tsipolitis[10], N. Tsirintanis[9], S. Tsiskaridze[12], V. Tsiskaridze[48], E.G. Tskhadadze[51a], I.I. Tsukerman[96], V. Tsulaia[15], S. Tsuno[65], D. Tsybychev[149], A. Tudorache[26a], V. Tudorache[26a], A.N. Tuna[121], S.A. Tupputi[20a,20b], S. Turchikhin[98,af], D. Turecek[127], I. Turk Cakir[4d], R. Turra[90a,90b], P.M. Tuts[35], A. Tykhonov[49], M. Tylmad[147a,147b], M. Tyndel[130], K. Uchida[21], I. Ueda[156], R. Ueno[29], M. Ughetto[84], M. Ugland[14], M. Uhlenbrock[21], F. Ukegawa[161], G. Unal[30], A. Undrus[25], G. Unel[164], F.C. Ungaro[48], Y. Unno[65], C. Unverdorben[99], D. Urbaniec[35], P. Urquijo[87], G. Usai[8], A. Usanova[61], L. Vacavant[84], V. Vacek[127], B. Vachon[86], N. Valencic[106], S. Valentinetti[20a,20b], A. Valero[168], L. Valery[34], S. Valkar[128], E. Valladolid Gallego[168], S. Vallecorsa[49], J.A. Valls Ferrer[168], W. Van Den Wollenberg[106],

P.C. Van Der Deijl[106], R. van der Geer[106], H. van der Graaf[106], R. Van Der Leeuw[106], D. van der Ster[30], N. van Eldik[30], P. van Gemmeren[6], J. Van Nieuwkoop[143], I. van Vulpen[106], M.C. van Woerden[30], M. Vanadia[133a,133b], W. Vandelli[30], R. Vanguri[121], A. Vaniachine[6], P. Vankov[42], F. Vannucci[79], G. Vardanyan[178], R. Vari[133a], E.W. Varnes[7], T. Varol[85], D. Varouchas[79], A. Vartapetian[8], K.E. Varvell[151], F. Vazeille[34], T. Vazquez Schroeder[54], J. Veatch[7], F. Veloso[125a,125c], T. Velz[21], S. Veneziano[133a], A. Ventura[72a,72b], D. Ventura[85], M. Venturi[170], N. Venturi[159], A. Venturini[23], V. Vercesi[120a], M. Verducci[133a,133b], W. Verkerke[106], J.C. Vermeulen[106], A. Vest[44], M.C. Vetterli[143,e], O. Viazlo[80], I. Vichou[166], T. Vickey[146c,ai], O.E. Vickey Boeriu[146c], G.H.A. Viehhauser[119], S. Viel[169], R. Vigne[30], M. Villa[20a,20b], M. Villaplana Perez[90a,90b], E. Vilucchi[47], M.G. Vincter[29], V.B. Vinogradov[64], J. Virzi[15], I. Vivarelli[150], F. Vives Vaque[3], S. Vlachos[10], D. Vladoiu[99], M. Vlasak[127], A. Vogel[21], M. Vogel[32a], P. Vokac[127], G. Volpi[123a,123b], M. Volpi[87], H. von der Schmitt[100], H. von Radziewski[48], E. von Toerne[21], V. Vorobel[128], K. Vorobev[97], M. Vos[168], R. Voss[30], J.H. Vossebeld[73], N. Vranjes[137], M. Vranjes Milosavljevic[106], V. Vrba[126], M. Vreeswijk[106], T. Vu Anh[48], R. Vuillermet[30], I. Vukotic[31], Z. Vykydal[127], P. Wagner[21], W. Wagner[176], H. Wahlberg[70], S. Wahrmund[44], J. Wakabayashi[102], J. Walder[71], R. Walker[99], W. Walkowiak[142], R. Wall[177], P. Waller[73], B. Walsh[177], C. Wang[152,aj], C. Wang[45], F. Wang[174], H. Wang[15], H. Wang[40], J. Wang[42], J. Wang[33a], K. Wang[86], R. Wang[104], S.M. Wang[152], T. Wang[21], X. Wang[177], C. Wanotayaroj[115], A. Warburton[86], C.P. Ward[28], D.R. Wardrope[77], M. Warsinsky[48], A. Washbrook[46], C. Wasicki[42], P.M. Watkins[18], A.T. Watson[18], I.J. Watson[151], M.F. Watson[18], G. Watts[139], S. Watts[83], B.M. Waugh[77], S. Webb[83], M.S. Weber[17], S.W. Weber[175], J.S. Webster[31], A.R. Weidberg[119], P. Weigell[100], B. Weinert[60], J. Weingarten[54], C. Weiser[48], H. Weits[106], P.S. Wells[30], T. Wenaus[25], D. Wendland[16], Z. Weng[152,ae], T. Wengler[30], S. Wenig[30], N. Wermes[21], M. Werner[48], P. Werner[30], M. Wessels[58a], J. Wetter[162], K. Whalen[29], A. White[8], M.J. White[1], R. White[32b], S. White[123a,123b], D. Whiteson[164], D. Wicke[176], F.J. Wickens[130], W. Wiedenmann[174], M. Wielers[130], P. Wienemann[21], C. Wiglesworth[36], L.A.M. Wiik-Fuchs[21], P.A. Wijeratne[77], A. Wildauer[100], M.A. Wildt[42,ak], H.G. Wilkens[30], J.Z. Will[99], H.H. Williams[121], S. Williams[28], C. Willis[89], S. Willocq[85], A. Wilson[88], J.A. Wilson[18], I. Wingerter-Seez[5], F. Winklmeier[115], B.T. Winter[21], M. Wittgen[144], T. Wittig[43], J. Wittkowski[99], S.J. Wollstadt[82], M.W. Wolter[39], H. Wolters[125a,125c], B.K. Wosiek[39], J. Wotschack[30], M.J. Woudstra[83], K.W. Wozniak[39], M. Wright[53], M. Wu[55], S.L. Wu[174], X. Wu[49], Y. Wu[88], E. Wulf[35], T.R. Wyatt[83], B.M. Wynne[46], S. Xella[36], M. Xiao[137], D. Xu[33a], L. Xu[33b,al], B. Yabsley[151], S. Yacoob[146b,am], R. Yakabe[66], M. Yamada[65], H. Yamaguchi[156], Y. Yamaguchi[117], A. Yamamoto[65], K. Yamamoto[63], S. Yamamoto[156], T. Yamamura[156], T. Yamanaka[156], K. Yamauchi[102], Y. Yamazaki[66], Z. Yan[22], H. Yang[33e], H. Yang[174], U.K. Yang[83], Y. Yang[110], S. Yanush[92], L. Yao[33a], W-M. Yao[15], Y. Yasu[65], E. Yatsenko[42], K.H. Yau Wong[21], J. Ye[40], S. Ye[25], I. Yeletskikh[64], A.L. Yen[57], E. Yildirim[42], M. Yilmaz[4b], R. Yoosoofmiya[124], K. Yorita[172], R. Yoshida[6], K. Yoshihara[156], C. Young[144], C.J.S. Young[30], S. Youssef[22], D.R. Yu[15], J. Yu[8], J.M. Yu[88], J. Yu[113], L. Yuan[66], A. Yurkewicz[107], I. Yusuff[28,an], B. Zabinski[39], R. Zaidan[62], A.M. Zaitsev[129,aa], A. Zaman[149], S. Zambito[23], L. Zanello[133a,133b], D. Zanzi[100], C. Zeitnitz[176], M. Zeman[127], A. Zemla[38a], K. Zengel[23], O. Zenin[129], T. Ženiš[145a], D. Zerwas[116], G. Zevi della Porta[57], D. Zhang[88], F. Zhang[174], H. Zhang[89], J. Zhang[6], L. Zhang[152], X. Zhang[33d], Z. Zhang[116], Z. Zhao[33b], A. Zhemchugov[64], J. Zhong[119], B. Zhou[88], L. Zhou[35], N. Zhou[164], C.G. Zhu[33d], H. Zhu[33a], J. Zhu[88], Y. Zhu[33b], X. Zhuang[33a], K. Zhukov[95], A. Zibell[175], D. Zieminska[60], N.I. Zimine[64], C. Zimmermann[82], R. Zimmermann[21], S. Zimmermann[21], S. Zimmermann[48], Z. Zinonos[54], M. Ziolkowski[142], G. Zobernig[174], A. Zoccoli[20a,20b], M. zur Nedden[16], G. Zurzolo[103a,103b], V. Zutshi[107], L. Zwalinski[30].

[1] Department of Physics, University of Adelaide, Adelaide, Australia
[2] Physics Department, SUNY Albany, Albany NY, United States of America
[3] Department of Physics, University of Alberta, Edmonton AB, Canada
[4] (a) Department of Physics, Ankara University, Ankara; (b) Department of Physics, Gazi University, Ankara; (c) Division of Physics, TOBB University of Economics and Technology, Ankara; (d) Turkish Atomic Energy Authority, Ankara, Turkey
[5] LAPP, CNRS/IN2P3 and Université de Savoie, Annecy-le-Vieux, France
[6] High Energy Physics Division, Argonne National Laboratory, Argonne IL, United States of America

[7] Department of Physics, University of Arizona, Tucson AZ, United States of America

[8] Department of Physics, The University of Texas at Arlington, Arlington TX, United States of America

[9] Physics Department, University of Athens, Athens, Greece

[10] Physics Department, National Technical University of Athens, Zografou, Greece

[11] Institute of Physics, Azerbaijan Academy of Sciences, Baku, Azerbaijan

[12] Institut de Física d'Altes Energies and Departament de Física de la Universitat Autònoma de Barcelona, Barcelona, Spain

[13] [a] Institute of Physics, University of Belgrade, Belgrade; [b] Vinca Institute of Nuclear Sciences, University of Belgrade, Belgrade, Serbia

[14] Department for Physics and Technology, University of Bergen, Bergen, Norway

[15] Physics Division, Lawrence Berkeley National Laboratory and University of California, Berkeley CA, United States of America

[16] Department of Physics, Humboldt University, Berlin, Germany

[17] Albert Einstein Center for Fundamental Physics and Laboratory for High Energy Physics, University of Bern, Bern, Switzerland

[18] School of Physics and Astronomy, University of Birmingham, Birmingham, United Kingdom

[19] [a] Department of Physics, Bogazici University, Istanbul; [b] Department of Physics, Dogus University, Istanbul; [c] Department of Physics Engineering, Gaziantep University, Gaziantep, Turkey

[20] [a] INFN Sezione di Bologna; [b] Dipartimento di Fisica e Astronomia, Università di Bologna, Bologna, Italy

[21] Physikalisches Institut, University of Bonn, Bonn, Germany

[22] Department of Physics, Boston University, Boston MA, United States of America

[23] Department of Physics, Brandeis University, Waltham MA, United States of America

[24] [a] Universidade Federal do Rio De Janeiro COPPE/EE/IF, Rio de Janeiro; [b] Electrical Circuits Department, Federal University of Juiz de Fora (UFJF), Juiz de Fora; [c] Federal University of Sao Joao del Rei (UFSJ), Sao Joao del Rei; [d] Instituto de Fisica, Universidade de Sao Paulo, Sao Paulo, Brazil

[25] Physics Department, Brookhaven National Laboratory, Upton NY, United States of America

[26] [a] National Institute of Physics and Nuclear Engineering, Bucharest; [b] National Institute for Research and Development of Isotopic and Molecular Technologies, Physics Department, Cluj Napoca; [c] University Politehnica Bucharest, Bucharest; [d] West University in Timisoara, Timisoara, Romania

[27] Departamento de Física, Universidad de Buenos Aires, Buenos Aires, Argentina

[28] Cavendish Laboratory, University of Cambridge, Cambridge, United Kingdom

[29] Department of Physics, Carleton University, Ottawa ON, Canada

[30] CERN, Geneva, Switzerland

[31] Enrico Fermi Institute, University of Chicago, Chicago IL, United States of America

[32] [a] Departamento de Física, Pontificia Universidad Católica de Chile, Santiago; [b] Departamento de Física, Universidad Técnica Federico Santa María, Valparaíso, Chile

[33] [a] Institute of High Energy Physics, Chinese Academy of Sciences, Beijing; [b] Department of Modern Physics, University of Science and Technology of China, Anhui; [c] Department of Physics, Nanjing University, Jiangsu; [d] School of Physics, Shandong University, Shandong; [e] Physics Department, Shanghai Jiao Tong University, Shanghai, China

[34] Laboratoire de Physique Corpusculaire, Clermont Université and Université Blaise Pascal and CNRS/IN2P3, Clermont-Ferrand, France

[35] Nevis Laboratory, Columbia University, Irvington NY, United States of America

[36] Niels Bohr Institute, University of Copenhagen, Kobenhavn, Denmark

[37] [a] INFN Gruppo Collegato di Cosenza, Laboratori Nazionali di Frascati; [b] Dipartimento di Fisica, Università della Calabria, Rende, Italy

[38] [a] AGH University of Science and Technology, Faculty of Physics and Applied Computer Science, Krakow; [b] Marian Smoluchowski Institute of Physics, Jagiellonian University, Krakow, Poland

[39] The Henryk Niewodniczanski Institute of Nuclear Physics, Polish Academy of Sciences, Krakow, Poland

[40] Physics Department, Southern Methodist University, Dallas TX, United States of America

[41] Physics Department, University of Texas at Dallas, Richardson TX, United States of America

[42] DESY, Hamburg and Zeuthen, Germany

[43] Institut für Experimentelle Physik IV, Technische Universität Dortmund, Dortmund, Germany

[44] Institut für Kern- und Teilchenphysik, Technische Universität Dresden, Dresden, Germany

[45] Department of Physics, Duke University, Durham NC, United States of America

[46] SUPA - School of Physics and Astronomy, University of Edinburgh, Edinburgh, United Kingdom

[47] INFN Laboratori Nazionali di Frascati, Frascati, Italy

[48] Fakultät für Mathematik und Physik, Albert-Ludwigs-Universität, Freiburg, Germany

[49] Section de Physique, Université de Genève, Geneva, Switzerland

[50] [a] INFN Sezione di Genova; [b] Dipartimento di Fisica, Università di Genova, Genova, Italy

[51] [a] E. Andronikashvili Institute of Physics, Iv. Javakhishvili Tbilisi State University, Tbilisi; [b] High Energy Physics Institute, Tbilisi State University, Tbilisi, Georgia

[52] II Physikalisches Institut, Justus-Liebig-Universität Giessen, Giessen, Germany

[53] SUPA - School of Physics and Astronomy, University of Glasgow, Glasgow, United Kingdom

[54] II Physikalisches Institut, Georg-August-Universität, Göttingen, Germany

[55] Laboratoire de Physique Subatomique et de Cosmologie, Université Grenoble-Alpes, CNRS/IN2P3, Grenoble, France

[56] Department of Physics, Hampton University, Hampton VA, United States of America

[57] Laboratory for Particle Physics and Cosmology, Harvard University, Cambridge MA, United States of America

[58] [a] Kirchhoff-Institut für Physik, Ruprecht-Karls-Universität Heidelberg, Heidelberg; [b] Physikalisches Institut, Ruprecht-Karls-Universität Heidelberg, Heidelberg; [c] ZITI Institut für technische Informatik, Ruprecht-Karls-Universität Heidelberg, Mannheim, Germany

[59] Faculty of Applied Information Science, Hiroshima Institute of Technology, Hiroshima, Japan

[60] Department of Physics, Indiana University, Bloomington IN, United States of America

[61] Institut für Astro- und Teilchenphysik, Leopold-Franzens-Universität, Innsbruck, Austria

[62] University of Iowa, Iowa City IA, United States of America

[63] Department of Physics and Astronomy, Iowa State University, Ames IA, United States of America

[64] Joint Institute for Nuclear Research, JINR Dubna, Dubna, Russia

[65] KEK, High Energy Accelerator Research Organization, Tsukuba, Japan

[66] Graduate School of Science, Kobe University, Kobe, Japan

[67] Faculty of Science, Kyoto University, Kyoto, Japan

[68] Kyoto University of Education, Kyoto, Japan

[69] Department of Physics, Kyushu University, Fukuoka, Japan

[70] Instituto de Física La Plata, Universidad Nacional de La Plata and CONICET, La Plata, Argentina

[71] Physics Department, Lancaster University, Lancaster, United Kingdom

[72] [a] INFN Sezione di Lecce; [b] Dipartimento di Matematica e Fisica, Università del Salento, Lecce, Italy

[73] Oliver Lodge Laboratory, University of Liverpool, Liverpool, United Kingdom

[74] Department of Physics, Jožef Stefan Institute and University of Ljubljana, Ljubljana, Slovenia

[75] School of Physics and Astronomy, Queen Mary University of London, London, United Kingdom

[76] Department of Physics, Royal Holloway University of London, Surrey, United Kingdom

[77] Department of Physics and Astronomy, University College London, London, United Kingdom

[78] Louisiana Tech University, Ruston LA, United States of America

[79] Laboratoire de Physique Nucléaire et de Hautes Energies, UPMC and Université Paris-Diderot and CNRS/IN2P3, Paris, France

[80] Fysiska institutionen, Lunds universitet, Lund, Sweden

[81] Departamento de Fisica Teorica C-15, Universidad Autonoma de Madrid, Madrid, Spain

[82] Institut für Physik, Universität Mainz, Mainz, Germany

[83] School of Physics and Astronomy, University of Manchester, Manchester, United Kingdom

[84] CPPM, Aix-Marseille Université and CNRS/IN2P3, Marseille, France

[85] Department of Physics, University of Massachusetts, Amherst MA, United States of America

[86] Department of Physics, McGill University, Montreal QC, Canada

[87] School of Physics, University of Melbourne, Victoria, Australia

[88] Department of Physics, The University of Michigan, Ann Arbor MI, United States of America

[89] Department of Physics and Astronomy, Michigan State University, East Lansing MI, United States of America

[90] [a] INFN Sezione di Milano; [b] Dipartimento di Fisica, Università di Milano, Milano, Italy

[91] B.I. Stepanov Institute of Physics, National Academy of Sciences of Belarus, Minsk, Republic of Belarus

[92] National Scientific and Educational Centre for Particle and High Energy Physics, Minsk, Republic of Belarus

[93] Department of Physics, Massachusetts Institute of Technology, Cambridge MA, United States of America

[94] Group of Particle Physics, University of Montreal, Montreal QC, Canada

[95] P.N. Lebedev Institute of Physics, Academy of Sciences, Moscow, Russia

[96] Institute for Theoretical and Experimental Physics (ITEP), Moscow, Russia

[97] National Research Nuclear University MEPhI, Moscow, Russia

[98] D.V. Skobeltsyn Institute of Nuclear Physics, M.V. Lomonosov Moscow State University, Moscow, Russia

[99] Fakultät für Physik, Ludwig-Maximilians-Universität München, München, Germany

[100] Max-Planck-Institut für Physik (Werner-Heisenberg-Institut), München, Germany

[101] Nagasaki Institute of Applied Science, Nagasaki, Japan

[102] Graduate School of Science and Kobayashi-Maskawa Institute, Nagoya University, Nagoya, Japan

[103] [a] INFN Sezione di Napoli; [b] Dipartimento di Fisica, Università di Napoli, Napoli, Italy

[104] Department of Physics and Astronomy, University of New Mexico, Albuquerque NM, United States of America

[105] Institute for Mathematics, Astrophysics and Particle Physics, Radboud University Nijmegen/Nikhef, Nijmegen, Netherlands

[106] Nikhef National Institute for Subatomic Physics and University of Amsterdam, Amsterdam, Netherlands

[107] Department of Physics, Northern Illinois University, DeKalb IL, United States of America

[108] Budker Institute of Nuclear Physics, SB RAS, Novosibirsk, Russia

[109] Department of Physics, New York University, New York NY, United States of America

[110] Ohio State University, Columbus OH, United States of America

[111] Faculty of Science, Okayama University, Okayama, Japan

[112] Homer L. Dodge Department of Physics and Astronomy, University of Oklahoma, Norman OK, United States of America

[113] Department of Physics, Oklahoma State University, Stillwater OK, United States of America

[114] Palacký University, RCPTM, Olomouc, Czech Republic

[115] Center for High Energy Physics, University of Oregon, Eugene OR, United States of America

[116] LAL, Université Paris-Sud and CNRS/IN2P3, Orsay, France

[117] Graduate School of Science, Osaka University, Osaka, Japan

[118] Department of Physics, University of Oslo, Oslo, Norway

[119] Department of Physics, Oxford University, Oxford, United Kingdom

[120] [a] INFN Sezione di Pavia; [b] Dipartimento di Fisica, Università di Pavia, Pavia, Italy

[121] Department of Physics, University of Pennsylvania, Philadelphia PA, United States of America

[122] Petersburg Nuclear Physics Institute, Gatchina, Russia

[123] [a] INFN Sezione di Pisa; [b] Dipartimento di Fisica E. Fermi, Università di Pisa, Pisa, Italy

[124] Department of Physics and Astronomy, University of Pittsburgh, Pittsburgh PA, United States of America

[125] [a] Laboratorio de Instrumentacao e Fisica Experimental de Particulas - LIP, Lisboa; [b] Faculdade de Ciências, Universidade de Lisboa, Lisboa; [c] Department of Physics, University of Coimbra, Coimbra; [d] Centro de Física Nuclear da Universidade de Lisboa, Lisboa; [e] Departamento de Fisica, Universidade do Minho, Braga; [f] Departamento de Fisica Teorica y del Cosmos and CAFPE, Universidad de Granada, Granada (Spain); [g] Dep Fisica and CEFITEC of Faculdade de Ciencias e Tecnologia, Universidade Nova de Lisboa, Caparica, Portugal

[126] Institute of Physics, Academy of Sciences of the Czech Republic, Praha, Czech Republic

[127] Czech Technical University in Prague, Praha, Czech Republic

[128] Faculty of Mathematics and Physics, Charles University in Prague, Praha, Czech Republic

[129] State Research Center Institute for High Energy Physics, Protvino, Russia

[130] Particle Physics Department, Rutherford Appleton Laboratory, Didcot, United Kingdom

[131] Physics Department, University of Regina, Regina SK, Canada

[132] Ritsumeikan University, Kusatsu, Shiga, Japan

[133] [a] INFN Sezione di Roma; [b] Dipartimento di Fisica, Sapienza Università di Roma, Roma, Italy

[134] [a] INFN Sezione di Roma Tor Vergata; [b] Dipartimento di Fisica, Università di Roma Tor Vergata, Roma, Italy

[135] [a] INFN Sezione di Roma Tre; [b] Dipartimento di Matematica e Fisica, Università Roma Tre, Roma, Italy

[136] [a] Faculté des Sciences Ain Chock, Réseau Universitaire de Physique des Hautes Energies - Université Hassan II, Casablanca; [b] Centre National de l'Energie des Sciences Techniques Nucleaires, Rabat; [c] Faculté des Sciences Semlalia, Université Cadi Ayyad, LPHEA-Marrakech; [d] Faculté des Sciences, Université Mohamed Premier and LPTPM, Oujda; [e] Faculté des sciences, Université Mohammed V-Agdal, Rabat, Morocco

[137] DSM/IRFU (Institut de Recherches sur les Lois Fondamentales de l'Univers), CEA Saclay (Commissariat à l'Energie Atomique et aux Energies Alternatives), Gif-sur-Yvette, France

[138] Santa Cruz Institute for Particle Physics, University of California Santa Cruz, Santa Cruz CA, United States of America

[139] Department of Physics, University of Washington, Seattle WA, United States of America

[140] Department of Physics and Astronomy, University of Sheffield, Sheffield, United Kingdom

[141] Department of Physics, Shinshu University, Nagano, Japan

[142] Fachbereich Physik, Universität Siegen, Siegen, Germany

[143] Department of Physics, Simon Fraser University, Burnaby BC, Canada

[144] SLAC National Accelerator Laboratory, Stanford CA, United States of America

[145] [a] Faculty of Mathematics, Physics & Informatics, Comenius University, Bratislava; [b] Department of Subnuclear Physics, Institute of Experimental Physics of the Slovak Academy of Sciences, Kosice, Slovak Republic

[146] [a] Department of Physics, University of Cape Town, Cape Town; [b] Department of Physics, University of Johannesburg, Johannesburg; [c] School of Physics, University of the Witwatersrand, Johannesburg, South Africa

[147] [a] Department of Physics, Stockholm University; [b] The Oskar Klein Centre, Stockholm, Sweden

[148] Physics Department, Royal Institute of Technology, Stockholm, Sweden

[149] Departments of Physics & Astronomy and Chemistry, Stony Brook University, Stony Brook NY, United States of America

[150] Department of Physics and Astronomy, University of Sussex, Brighton, United Kingdom

[151] School of Physics, University of Sydney, Sydney, Australia

[152] Institute of Physics, Academia Sinica, Taipei, Taiwan

[153] Department of Physics, Technion: Israel Institute of Technology, Haifa, Israel

[154] Raymond and Beverly Sackler School of Physics and Astronomy, Tel Aviv University, Tel Aviv, Israel

[155] Department of Physics, Aristotle University of Thessaloniki, Thessaloniki, Greece

[156] International Center for Elementary Particle Physics and Department of Physics, The University of Tokyo, Tokyo, Japan

[157] Graduate School of Science and Technology, Tokyo Metropolitan University, Tokyo, Japan

[158] Department of Physics, Tokyo Institute of Technology, Tokyo, Japan

[159] Department of Physics, University of Toronto, Toronto ON, Canada

[160] [a] TRIUMF, Vancouver BC; [b] Department of Physics and Astronomy, York University, Toronto ON, Canada

[161] Faculty of Pure and Applied Sciences, University of Tsukuba, Tsukuba, Japan

[162] Department of Physics and Astronomy, Tufts University, Medford MA, United States of America

[163] Centro de Investigaciones, Universidad Antonio Narino, Bogota, Colombia

[164] Department of Physics and Astronomy, University of California Irvine, Irvine CA, United States of America

[165] [a] INFN Gruppo Collegato di Udine, Sezione di Trieste, Udine; [b] ICTP, Trieste; [c] Dipartimento di Chimica, Fisica e Ambiente, Università di Udine, Udine, Italy

[166] Department of Physics, University of Illinois, Urbana IL, United States of America

[167] Department of Physics and Astronomy, University of Uppsala, Uppsala, Sweden

[168] Instituto de Física Corpuscular (IFIC) and Departamento de Física Atómica, Molecular y Nuclear and Departamento de Ingeniería Electrónica and Instituto de Microelectrónica de Barcelona (IMB-CNM), University of Valencia and CSIC, Valencia, Spain

[169] Department of Physics, University of British Columbia, Vancouver BC, Canada

[170] Department of Physics and Astronomy, University of Victoria, Victoria BC, Canada

[171] Department of Physics, University of Warwick, Coventry, United Kingdom

[172] Waseda University, Tokyo, Japan

[173] Department of Particle Physics, The Weizmann Institute of Science, Rehovot, Israel

[174] Department of Physics, University of Wisconsin, Madison WI, United States of America

[175] Fakultät für Physik und Astronomie, Julius-Maximilians-Universität, Würzburg, Germany

[176] Fachbereich C Physik, Bergische Universität Wuppertal, Wuppertal, Germany

[177] Department of Physics, Yale University, New Haven CT, United States of America

[178] Yerevan Physics Institute, Yerevan, Armenia

[179] Centre de Calcul de l'Institut National de Physique Nucléaire et de Physique des Particules (IN2P3), Villeurbanne, France

[a] Also at Department of Physics, King's College London, London, United Kingdom

[b] Also at Institute of Physics, Azerbaijan Academy of Sciences, Baku, Azerbaijan

[c] Also at Novosibirsk State University, Novosibirsk, Russia

[d] Also at Particle Physics Department, Rutherford Appleton Laboratory, Didcot, United Kingdom

[e] Also at TRIUMF, Vancouver BC, Canada

[f] Also at Department of Physics, California State University, Fresno CA, United States of America

[g] Also at Department of Physics, University of Fribourg, Fribourg, Switzerland

[h] Also at Tomsk State University, Tomsk, Russia

[i] Also at CPPM, Aix-Marseille Université and CNRS/IN2P3, Marseille, France

[j] Also at Università di Napoli Parthenope, Napoli, Italy

[k] Also at Institute of Particle Physics (IPP), Canada

[l] Also at Department of Physics, St. Petersburg State Polytechnical University, St. Petersburg, Russia

[m] Also at Chinese University of Hong Kong, China

[n] Also at Louisiana Tech University, Ruston LA, United States of America

[o] Also at Institucio Catalana de Recerca i Estudis Avancats, ICREA, Barcelona, Spain

[p] Also at Department of Physics, The University of Texas at Austin, Austin TX, United States of America

[q] Also at Institute of Theoretical Physics, Ilia State University, Tbilisi, Georgia

[r] Also at CERN, Geneva, Switzerland

[s] Also at Ochadai Academic Production, Ochanomizu University, Tokyo, Japan

[t] Also at Manhattan College, New York NY, United States of America

[u] Also at Institute of Physics, Academia Sinica, Taipei, Taiwan

[v] Also at LAL, Université Paris-Sud and CNRS/IN2P3, Orsay, France

[w] Also at Academia Sinica Grid Computing, Institute of Physics, Academia Sinica, Taipei, Taiwan

[x] Also at Laboratoire de Physique Nucléaire et de Hautes Energies, UPMC and Université Paris-Diderot and CNRS/IN2P3, Paris, France

[y] Also at School of Physical Sciences, National Institute of Science Education and Research, Bhubaneswar, India

[z] Also at Dipartimento di Fisica, Sapienza Università di Roma, Roma, Italy

[aa] Also at Moscow Institute of Physics and Technology State University, Dolgoprudny, Russia

[ab] Also at Section de Physique, Université de Genève, Geneva, Switzerland

[ac] Also at International School for Advanced Studies (SISSA), Trieste, Italy

[ad] Also at Department of Physics and Astronomy, University of South Carolina, Columbia SC, United States of America

[ae] Also at School of Physics and Engineering, Sun Yat-sen University, Guangzhou, China

[af] Also at Faculty of Physics, M.V.Lomonosov Moscow State University, Moscow, Russia

[ag] Also at National Research Nuclear University MEPhI, Moscow, Russia

[ah] Also at Institute for Particle and Nuclear Physics, Wigner Research Centre for Physics, Budapest, Hungary

[ai] Also at Department of Physics, Oxford University, Oxford, United Kingdom

[aj] Also at Department of Physics, Nanjing University, Jiangsu, China

[ak] Also at Institut für Experimentalphysik, Universität Hamburg, Hamburg, Germany

[al] Also at Department of Physics, The University of Michigan, Ann Arbor MI, United States of America

[am] Also at Discipline of Physics, University of KwaZulu-Natal, Durban, South Africa

[an] Also at University of Malaya, Department of Physics, Kuala Lumpur, Malaysia

* Deceased